

# Spherical Regression under Mismatch Corruption with Application to Automated Knowledge Translation

Xu Shi<sup>1</sup>, Xiaoou Li<sup>2</sup>, and Tianxi Cai<sup>1</sup>

<sup>1</sup>Department of Biostatistics, Harvard University

<sup>2</sup>Department of Statistics, University of Minnesota

## Abstract

Motivated by a series of applications in data integration, language translation, bioinformatics, and computer vision, we consider spherical regression with two sets of unit-length vectors when the data are corrupted by a small fraction of mismatch in the response-predictor pairs. We propose a three-step algorithm in which we initialize the parameters by solving an orthogonal Procrustes problem to estimate a translation matrix  $\mathbb{W}$  ignoring the mismatch. We then estimate a mapping matrix aiming to correct the mismatch using hard-thresholding to induce sparsity, while incorporating potential group information. We eventually obtain a refined estimate for  $\mathbb{W}$  by removing the estimated mismatched pairs. We derive the error bound for the initial estimate of  $\mathbb{W}$  in both fixed and high-dimensional setting. We demonstrate that the refined estimate of  $\mathbb{W}$  achieves an error rate that is as good as if no mismatch is present. We show that our mapping recovery method not only correctly distinguishes one-to-one and one-to-many correspondences, but also consistently identifies the matched pairs and estimates the weight vector for combined correspondence. We examine the finite sample performance of the proposed method via extensive simulation studies, and with application to the unsupervised translation of medical codes using electronic health records data.

*Keywords:* electronic health records, hard-thresholding, mismatched data, ontology translation, spherical regression

# 1 Introduction

Classical multivariate regression analysis studies the relationship between a response random vector and a predictor random vector, under the assumptions that the response-predictor pairs are correctly linked, and that the data lies in an unrestricted Euclidean space. However, modern large-scale datasets are frequently integrated from multiple heterogeneous data sources. Observations from different datasets are often imperfectly matched due to linkage error. In addition, in many real-world settings ranging from gene expression analysis to language processing, the response and predictor vectors represent directional data, which lie on the surface of a hypersphere (Gotsman et al. 2003, Xing et al. 2015). Motivated by the applications in the automated translation of medical code, we propose in this paper novel multivariate regression procedures for spherical data in the presence of mismatch. We first detail the motivating examples and then discuss the statistical contributions of the paper.

## 1.1 Automated translation of medical codes

The Centers for Medicare and Medicaid Services (CMS) recently renamed the EHR Incentive Program from “meaningful use” to “promoting interoperability”, aiming to improve the integration and sharing of health information among providers, clinicians, and patients. A key challenge is the lack of semantic interoperability because the “languages” used in different EHR systems and across time may be inconsistent. For example, the International Classification of Diseases (ICD) codes describe medical diagnoses and procedures for billing and administrative purposes. Data on ICD codes are used extensively for biomedical research (Yu et al. 2015, Chen et al. 2013, Parle et al. 2001, e.g). However, due to the coding incentives and the heterogeneity in healthcare systems, different providers may use alternative codes to record the same diagnosis or procedure, limiting the transportability of phenotyping algorithms and prediction models across systems. Translation between ICD codes used in different healthcare systems can potentially overcome such challenges.

Another example of code translation arises from the updating of ICD coding systems. All U.S. healthcare systems are federally mandated in 2015 to replace the 9th edition of ICD (ICD-9) codes with the 10th edition (ICD-10) codes for all claims of service, with a potential to convert to the 11th edition in 2022 (World Health Organization 2018). Mappings

between ICD-9 and ICD-10 codes are essential for linking and analyzing EHR data before and after the transition. Available manual annotations including the General Equivalence Mappings (GEM) are intrinsically ambiguous due to the increase in number (over 700% more than ICD-9 codes) and complexity of ICD-10 codes (Krive et al. 2015). In particular, a significant portion of the GEM mappings are one-to-many mapping, and many are approximate matches. For example, the ICD-9 code 995.29 “*unspecified adverse effect of other drug, medicinal and biological substance*” is mapped to over a hundred ICD-10 codes. The presence of one-to-many mapping and the inherent differences between the two coding systems pose substantial challenges to the translation of ICD-9 codes to ICD-10 codes.

Manual translation of medical codes is not only immensely laborious but also error prone, signifying the need for data-driven translation methods. In this paper, we turn the problem of code translation into a statistical problem of mapping two sets of unit-length vectors,  $\mathbb{Y} = [\mathbf{Y}_1, \dots, \mathbf{Y}_n]^\top$  from one system and  $\mathbb{X} = [\mathbf{X}_1, \dots, \mathbf{X}_n]^\top$  from another system, where  $\mathbf{Y}_i$  and  $\mathbf{X}_i$  respectively represent semantic embedding vector (SEV) for the  $i^{th}$  code in the two systems. The code SEVs were generated from co-occurrence patterns of ICD codes using word embedding algorithms such as `word2vec` (Mikolov et al. 2013). See Beam et al. (2018) for details on generating SEVs using patient level ICD code data. The directions of the SEVs encode the relationship, similarity, and clinical meanings of the codes. Particularly, the SEVs of codes with more similar meanings are closer to each other. We thus propose to achieve code translation by inferring a mapping between the embeddings,  $\mathbb{Y}$  and  $\mathbb{X}$ .

In addition to medical code translation, regression with mismatched spherical data have applications in many other scientific problems. Examples include language processing (Xing et al. 2015, Wilson & Schakel 2015), bioinformatics (Sael & Kihara 2010, Samarov et al. 2011), pose and correspondence determination in image processing (Gold et al. 1995, Zhou et al. 2014), simultaneous localization and mapping in robotics (Kaess 2015, Esteves et al. 2018), shape matching and retrieval (Kazhdan et al. 2003, Papadakis et al. 2007) and computer vision and pattern recognition (Marques et al. 2009, Cohen et al. 2018).

## 1.2 Spherical Regression with Mismatched Data

We propose to create a mapping between the code SEVs allowing for both one-to-one and one-to-many correspondences by developing a spherical regression model with mismatched

data. Specifically, we assume that  $\mathbf{Y}_i$  relates to  $\mathbb{X} = [\mathbf{X}_1, \dots, \mathbf{X}_n]^\top$  only through  $(\mathbf{\Pi}_i \mathbb{X} \mathbb{W})^\top$ , where  $\mathbf{X}_i$  and  $\mathbf{Y}_i$  lie on the surface of a  $p$ -dimensional unit sphere denoted by  $\mathcal{S}^{p-1}$ ,  $\mathbb{W} \in \mathcal{R}^{p \times p}$  is an orthogonal translation matrix satisfying  $\mathbb{W} \mathbb{W}^\top = \mathbb{I}_p$  with  $\mathbb{I}_p$  an identity matrix, and  $\mathbf{\Pi} = [\mathbf{\Pi}_1^\top, \dots, \mathbf{\Pi}_n^\top]^\top \in \mathcal{R}^{n \times n}$  is a mapping matrix that corrects the potential mismatch.

There is a growing literature on the regression problem of  $\mathbf{Y}_i = (\mathbf{\Pi}_i \mathbb{X} \mathbb{W})^\top + \mathbf{U}_i$  when  $\mathbf{\Pi}$  is a *permutation* matrix encoding only one-to-one correspondence between  $\mathbb{X}$  and  $\mathbb{Y}$  and no orthogonality constraint is imposed on  $\mathbb{W}$  (Pananjady et al. 2017a,b, Slawski & Ben-David 2017, Abid et al. 2017, Hsu et al. 2017, Unnikrishnan et al. 2018, e.g.). It has been shown that the least squares estimator of  $\mathbb{W}$  is generally inconsistent without any additional constraints imposed on  $\mathbf{\Pi}$  (Pananjady et al. 2017a,b, Slawski & Ben-David 2017). When  $\mathbf{\Pi}$  is sparse in that only a small portion of the responses or predictors is permuted,  $\mathbb{W}$  can be consistently estimated (Slawski & Ben-David 2017). Algorithms for estimation of  $\mathbb{W}$  have also been studied (Hsu et al. 2017, Abid et al. 2017, Unnikrishnan et al. 2018). Estimation of the permutation matrix  $\mathbf{\Pi}$  is challenging both computationally and statistically. Specifically, permutation recovery is generally NP-hard unless  $p = 1$  or  $\mathbf{U}_i = 0$  (Pananjady et al. 2017b, Hsu et al. 2017). When  $p = 1$ , estimation of  $\mathbf{\Pi}$  reduces to a sorting problem and thus is computationally tractable. Statistical limit in terms of conditions on the signal-to-noise ratio (SNR) required for the recovery of  $\mathbf{\Pi}$  has also been studied (Pananjady et al. 2017b, Slawski & Ben-David 2017, Hsu et al. 2017).

Existing literature on multivariate regression with mismatched data generally assumes Gaussian data with a random or fixed design matrix, while this paper concerns the case where both  $\mathbf{X}_i$  and  $\mathbf{Y}_i$  belong to  $\mathcal{S}^{p-1}$ . With perfectly matched data in the spherical domain  $\mathcal{S}^{p-1}$ , estimation of an orthogonal matrix  $\mathbb{W} \in SO(p) = \{A \in \mathcal{R}^{p \times p} : AA^\top = \mathbb{I}_p\}$  that transforms the predictors to responses has been referred to as the spherical regression in the literature (Chang 1986, 1989, Goodall 1991, Kim et al. 1998, Rosenthal et al. 2014, Di Marzio et al. 2018). Statistical inference beyond the classical setup of fixed dimension  $p$  has also been considered recently (Paindaveine & Verdebout 2017). However, the current literature is based on the assumption that the response and predictor are correctly linked.

In this paper, we fill the gap by developing estimation procedures for  $\mathbb{W}$  and  $\mathbf{\Pi}$  with mismatched spherical data. Instead of imposing one-to-one correspondence for  $\mathbf{\Pi}$ , we focus on the setting where  $\mathbf{\Pi}$  is sparse with a block diagonal structure allowing for both one-to-one

and one-to-many mappings. Specifically, we assume that the group information on the codes is available and mismatch is only expected to occur within a group. In the ICD example, codes within the same group representing very different diseases, for example rheumatoid arthritis versus type II diabetes, are unlikely to be used exchangeably across healthcare systems. Such structure may not ease estimation of  $\mathbb{W}$  but can greatly reduce the difficulty in recovering  $\mathbf{\Pi}$ . To the best of our knowledge, no existing method consider the recovery of a general mapping matrix leveraging group information. The rest of the paper is organized as follows. We detail our model assumptions and estimation procedures in Section 2. In Section 3, we investigate how the degree of mismatch influences the error rates, and we detail theoretical guarantees for our proposed method. We evaluate the performance of our proposed method via extensive simulation studies in Section 4. In Section 5 we apply the proposed method to translate ICD-9 codes between two healthcare systems using SEV data derived from the two corresponding EHRs and to translate between ICD-9 and ICD-10 codes using SEV data derived from the same EHR system. We close with a discussion in Section 6.

## 2 Method

### 2.1 Notations

We assume that the data consists of  $n$  pairs of  $p$ -dimensional unit-length vectors in  $\mathbb{S}^{p-1}$ , i.e.,  $\mathbb{Y} = [Y_{ik}]_{n \times p} = [\mathbf{Y}_1, \dots, \mathbf{Y}_n]^\top$  and  $\mathbb{X} = [X_{ik}]_{n \times p} = [\mathbf{X}_1, \dots, \mathbf{X}_n]^\top$ . The  $n$  observations belong to  $K$  groups indexed by  $\{G_1, \dots, G_K\} \subset [n] = \{1, \dots, n\}$  and mismatch only occurs within group. Let  $n_k = |G_k|$  denote the group size with  $\sum_{k=1}^K n_k = n$ , where for an index set  $G$ ,  $|G|$  denotes its cardinality. Without loss of generality, we assume that the data is ordered by group and thus  $\mathbf{\Pi} = \text{diag}\{\mathbf{\Pi}^1, \dots, \mathbf{\Pi}^K\}$ , where  $\mathbf{\Pi}^k$  denotes the matrix that encodes the mapping among records within  $G_k$ . For indexes  $i, j \in [n]$ , let  $i \sim j$  denote that  $i$  and  $j$  belong to the same group, i.e.,  $i, j \in G_k$  for some  $k$ .

For a matrix  $\mathbf{A}$ , let  $\mathbf{A}_{i\cdot}$  and  $\mathbf{A}_{\cdot j}$  respectively denote its  $i^{\text{th}}$  row and  $j^{\text{th}}$  column,  $\sigma_i(\mathbf{A})$  denote the  $i^{\text{th}}$  largest singular value of  $\mathbf{A}$ , and  $\|\mathbf{A}\|_F$  denote the Frobenius norm of  $\mathbf{A}$ . For an index set  $G$ , let  $\mathbf{A}_{[G, :]}$  denote the rows of  $\mathbf{A}$  corresponding to  $G$ . Let  $\|\cdot\|_2$  denote the  $\ell_2$  norm of a vector. Let  $\mathbb{I}_n$  denote the  $n \times n$  identity matrix, and we omit  $n$  when it is

self-explanatory. For any mapping matrix  $\boldsymbol{\pi} \in \mathcal{R}^{n \times n}$ , let  $\mathcal{S}(\boldsymbol{\pi}) = \{i \in [n] : \boldsymbol{\pi}_i = \mathbb{I}_i\}$  and  $\mathcal{D}(\mathbb{I}, \boldsymbol{\pi}) = \{i \in [n] : \mathbb{I}_i \neq \boldsymbol{\pi}_i\}$  respectively index the set of matched and mismatched units as determined by  $\boldsymbol{\pi}$ . Accordingly, let  $n_{\text{mis}} = |\mathcal{D}(\mathbb{I}, \boldsymbol{\Pi})|$  denote the number of mismatched pairs in the data. For any set  $\mathcal{S}$ ,  $\mathcal{S}^c$  denotes its complement.

## 2.2 Model Assumptions

### 2.2.1 Spherical data and the von-Mises Fisher distribution

Unlike the Euclidean space, the  $\mathcal{S}^{p-1}$  sample space features distinctive characteristics both theoretically and practically. The most widely used distribution family for random vectors in  $\mathcal{S}^{p-1}$  is the von-Mises Fisher (vMF) distribution. The  $p$ -dimensional vMF distribution with parameters  $\boldsymbol{\mu}$  and  $\kappa$ , denoted by  $\text{vMF}_{\boldsymbol{\mu}, \kappa, p}$ , has density

$$f_{\text{vMF}}(\mathbf{Y} | \boldsymbol{\mu}; \kappa) = C_p(\kappa) \exp(\kappa \boldsymbol{\mu}^\top \mathbf{Y}) = C_p(\kappa) \exp\{\kappa \cos(\boldsymbol{\mu}, \mathbf{Y})\}, \quad (1)$$

where  $\kappa \geq 0$  is a concentration parameter,  $\boldsymbol{\mu} \in \mathcal{R}^p$  is the mean direction with  $\|\boldsymbol{\mu}\|_2 = 1$ ,  $C_p(\kappa) = \kappa^{p/2-1} / \{(2\pi)^{p/2} B_{p/2-1}(\kappa)\}$ , and  $B_{p/2-1}(\cdot)$  denotes the modified Bessel function of order  $p/2 - 1$ . The vMF distribution belongs to the exponential family and thus has many desirable statistical properties. For example, one can show that if  $\mathbf{Z} \sim N(\boldsymbol{\mu}, \mathbb{I}_p/\kappa)$ , then conditional on having unit length,  $\mathbf{Z} | \|\mathbf{Z}\|_2 = 1$  follows  $\text{vMF}_{\boldsymbol{\mu}, \kappa, p}$  distribution. In addition, for a random vector  $\mathbf{Y} \sim \text{vMF}_{\boldsymbol{\mu}, \kappa, p}$ , we have  $E[\mathbf{Y}] = \gamma_{\kappa, p} \boldsymbol{\mu}$  and  $E[\|\mathbf{Y} - E[\mathbf{Y}]\|_2^2] = 1 - \gamma_{\kappa, p}^2$ , where  $\gamma_{\kappa, p} = B'_{p/2-1}(\kappa) / B_{p/2-1}(\kappa) - (p/2 - 1)/\kappa$  can be bounded as in the following lemma:

**Lemma 1.** For  $p \geq 4$  and  $\kappa > 0$ ,  $\max\{0, 1 - \frac{p-1}{2\kappa}\} < \gamma_{\kappa, p} < 1$ .

The above results are proved in Section C of the supplementary material. Intuitively, random vectors following the  $\text{vMF}_{\boldsymbol{\mu}, \kappa, p}$  distribution are symmetrically distributed on  $\mathcal{S}^{p-1}$  concentrating around the mean direction  $\boldsymbol{\mu}$ . The expectation is of the same direction as  $\boldsymbol{\mu}$  but lies inside the sphere, i.e.,  $\gamma_{\kappa, p} < 1$ . As the distribution gets more concentrated around  $\boldsymbol{\mu}$ , the expectation gets closer to  $\boldsymbol{\mu}$ . The large deviation bounds for sums of i.i.d copies of  $\|\mathbf{Y} - \boldsymbol{\mu}\|_2^2$ , derived in Proposition A.1 of the supplementary material, may be of independent interest.

### 2.2.2 Unified loss function on the hypersphere

The spherical data is also unique in that the loss function defined on the hypersphere unifies a lot of commonly used distance measures. Here we formally introduce our objective function for estimating  $\mathbb{W}$  and illustrate such unifying property. To ease exposition, we first consider a simplified scenario with  $\mathbf{\Pi} = \mathbb{I}_n$  under which we may estimate the translation matrix  $\mathbb{W}$  by minimizing the Frobenius norm

$$\widehat{\mathbb{W}} = \underset{\mathbb{W}: \mathbb{W}\mathbb{W}^\top = \mathbb{I}_p}{\operatorname{argmin}} \widehat{\ell}_0(\mathbb{W}), \text{ where } \widehat{\ell}_0(\mathbb{W}) = \|\mathbb{Y} - \mathbb{X}\mathbb{W}\|_F^2. \quad (2)$$

The role of  $\mathbb{W}$  is to align the spaces spanned by columns of  $\mathbb{X}$  and  $\mathbb{Y}$  such that samples in  $\mathbb{Y}$  and  $\mathbb{X}\mathbb{W}$  can be compared in distance. The orthogonal parameterization  $\mathbb{W}\mathbb{W}^\top = \mathbb{I}$  ensures that the transformed data remains on the sphere, i.e.  $\|\mathbb{W}^\top \mathbf{X}_i\|_2 = \|\mathbf{X}_i\|_2 = 1$ .

Because both  $\mathbf{X}_i$  and  $\mathbf{Y}_i$  have unit length, minimizing the loss function is equivalent to maximizing the cosine similarities between  $\mathbf{Y}_i$  and its transformed counterpart  $\mathbb{W}^\top \mathbf{X}_i$ . In addition, the cosine similarity is equal to the inner product when the vectors are of unit lengths. To summarize, we have the following equivalence

$$\underset{\mathbb{W}: \mathbb{W}\mathbb{W}^\top = \mathbb{I}_p}{\operatorname{argmin}} \widehat{\ell}_0(\mathbb{W}) = \underset{\mathbb{W}: \mathbb{W}\mathbb{W}^\top = \mathbb{I}_p}{\operatorname{argmax}} \sum_{i=1}^n \cos(\mathbf{Y}_i, \mathbb{W}^\top \mathbf{X}_i) = \underset{\mathbb{W}: \mathbb{W}\mathbb{W}^\top = \mathbb{I}_p}{\operatorname{argmax}} \sum_{i=1}^n \mathbf{Y}_i^\top \cdot (\mathbb{W}^\top \mathbf{X}_i).$$

The loss function  $\widehat{\ell}_0(\mathbb{W})$  also corresponds to the log-likelihood function under the vMF distribution. Specifically,  $\widehat{\ell}_0(\mathbb{W})$  corresponds to the log-likelihood function under the model

$$f_{\text{vMF}}(\mathbf{Y}_i | \mathbb{X}; \kappa) = C_p(\kappa) \exp(\kappa \boldsymbol{\mu}_i^\top \mathbf{Y}_i) \quad \text{with} \quad \boldsymbol{\mu}_i = \mathbb{W}^\top \mathbf{X}_i = \mathbb{W}^\top (\mathbb{I}_i \mathbb{X})^\top \text{ and } \mathbb{W}\mathbb{W}^\top = \mathbb{I}_p \quad (3)$$

with  $\mathbf{Y}_i | \mathbb{X}, i \in [n]$  independent. We thus target an objective on the hypersphere  $\mathcal{S}^{p-1}$  unifying the Frobenius norm, the cosine similarity, the inner product, and the likelihood function of the von Mises-Fisher distribution.

### 2.2.3 Model Assumptions under Mismatch with Group Structure

Building upon the above objective, we consider the general scenario in the presence of mismatch with  $\mathbf{\Pi} \neq \mathbb{I}_n$ . Estimating  $\mathbf{\Pi}$  and  $\mathbb{W}$  without any constraint is infeasible due to the

large number of parameters. In addition to  $\mathbf{\Pi}$  being block diagonal, we assume that only a small fraction of mismatch occurs and hence  $n_{\text{mis}} = o(n)$ . However, we do not constrain  $\mathbf{\Pi}$  to be a permutation matrix and accommodate more complex mismatch patterns. For example, if  $\mathbf{X}$  and  $\mathbf{Y}$  represent ICD-10 and ICD-9 codes respectively,  $\mathbf{Y}_i$  may not be mapped to any single ICD-10 code but rather needs to be represented by a combination of multiple ICD-10 codes in  $\mathbb{X}$ . We also allow some columns of  $\mathbf{\Pi}$  to be zero vectors, indicating that the corresponding unit of  $\mathbb{X}$  does not link to any response in  $\mathbb{Y}$ . In the presence of mismatch, we assume that  $\mathbf{Y}_i \mid \mathbb{X}$  are independent and follows

$$f_{\text{vMF}}(\mathbf{Y}_i \mid \mathbb{X}; \kappa) = C_p(\kappa) \exp(\kappa \boldsymbol{\mu}_{\mathbf{\Pi},i}^\top \mathbf{Y}_i) \quad \text{with} \quad \boldsymbol{\mu}_{\mathbf{\Pi},i} = \mathbb{W}^\top (\mathbf{\Pi}_i \mathbb{X})^\top, \quad \mathbb{W} \mathbb{W}^\top = \mathbb{I}_p \quad (4)$$

and  $\|(\mathbf{\Pi}_i \mathbb{X})^\top\|_2 = 1$  to ensure that the mapped vector  $(\mathbf{\Pi}_i \mathbb{X})^\top$  remains on  $\mathcal{S}^{p-1}$ . A necessary condition for  $\|(\mathbf{\Pi}_i \mathbb{X})^\top\|_2 = 1$  is  $\frac{1}{\sqrt{n_k}} \leq \|\mathbf{\Pi}_i\|_2 \leq \frac{1}{\sigma_{n_k}(\mathbb{X}_{[G_k, :]})}$ , for all  $i \in G_k$ , which is shown in Lemma C.4. We further assume that  $n > p > \max_{1 \leq k \leq K} n_k$  and  $\kappa \neq 0$ .

## 2.3 Iterative spherical regression mapping (iSphereMAP)

We propose an iterative spherical regression mapping (iSphereMAP) method to estimate the translation matrix  $\mathbb{W}$  and the mapping matrix  $\mathbf{\Pi}$ . Although the iSphereMAP procedure can iterate until convergence, we find that the estimators stabilize after three steps and hence focus on the three-step procedure. In step I, we simply estimate  $\mathbf{\Pi}$  as  $\hat{\mathbf{\Pi}}^{[1]} = \mathbb{I}_n$  and obtain an initial estimator for  $\mathbb{W}$  as

$$\widehat{\mathbb{W}}^{[1]} = \underset{\mathbb{W}: \mathbb{W} \mathbb{W}^\top = \mathbb{I}_p}{\text{argmin}} \|\mathbb{Y}_{[\mathcal{S}(\hat{\mathbf{\Pi}}^{[1]})],:} - \mathbb{X}_{[\mathcal{S}(\hat{\mathbf{\Pi}}^{[1]})],:} \mathbb{W}\|_F^2 = \underset{\mathbb{W}: \mathbb{W} \mathbb{W}^\top = \mathbb{I}_p}{\text{argmin}} \|\mathbb{Y} - \mathbb{X} \mathbb{W}\|_F^2 = \underset{\mathbb{W}: \mathbb{W} \mathbb{W}^\top = \mathbb{I}_p}{\text{argmin}} \widehat{\ell}_0(\mathbb{W}). \quad (5)$$

The degree of mismatch between  $\hat{\mathbf{\Pi}}^{[1]}$  and the true  $\mathbf{\Pi}$  is of size  $n_{\text{mis}} = n - |\mathcal{S}(\mathbf{\Pi})|$  with  $\mathcal{D}(\mathbb{I}, \mathbf{\Pi}) = \mathcal{S}(\mathbf{\Pi})^c$ . Solving for  $\mathbb{W}$  in the optimization problem (5) is a well-known orthogonal Procrustes problem (Schönemann 1966, Gower et al. 2004, e.g.), the solution to which is the polar decomposition of  $\mathbb{X}^\top \mathbb{Y}$  (Higham 1986, e.g.):

$$\widehat{\mathbb{W}}^{[1]} = \mathcal{U}(\mathbb{X}^\top \mathbb{Y}), \quad \text{where for any nonsingular matrix } \mathbb{A}_{p \times p}, \mathcal{U}(\mathbb{A}) = \mathbb{A}(\mathbb{A}^\top \mathbb{A})^{-\frac{1}{2}}.$$



In step II, we obtain an improved estimator of  $\mathbf{\Pi}$  by mapping the translated data,  $\mathbb{Y}$  and  $\mathbb{X}\widehat{\mathbb{W}}^{[1]}$ . Recall that  $\mathbf{\Pi} = \text{diag}\{\mathbf{\Pi}^1, \dots, \mathbf{\Pi}^k\}$ , where the mapping matrix for the  $k^{\text{th}}$  group,  $\mathbf{\Pi}^k$ , is an  $n_k \times n_k$  matrix. We estimate each  $\mathbf{\Pi}^k$  using a hard-thresholding procedure as follows. First, we compute an initial estimate  $\widetilde{\mathbf{\Pi}}^k$  by the ordinary least squares (OLS) as

$$\widetilde{\mathbf{\Pi}}^k = \mathbb{Y}_{[G_k, :]} (\mathbb{X}_{[G_k, :]} \widehat{\mathbb{W}}^{[1]})^\top (\mathbb{X}_{[G_k, :]} \mathbb{X}_{[G_k, :]}^\top)^{-1}.$$

Then to obtain a sparse estimate of  $\mathbf{\Pi}$ , we apply hard-thresholding to  $\widetilde{\mathbf{\Pi}} = \text{diag}\{\widetilde{\mathbf{\Pi}}^1, \dots, \widetilde{\mathbf{\Pi}}^K\}$  allowing for one-to-many correspondence within group. Specifically, for each  $i \in [n]$ , let

$$\beta_i = 1 - \max_{j: j \sim i} \cos(\mathbf{\Pi}_i, \mathbb{I}_j), \quad \widetilde{\beta}_i = 1 - \max_{j: j \sim i} \cos(\widetilde{\mathbf{\Pi}}_i, \mathbb{I}_j), \quad \text{and} \quad \widetilde{j}_i = \arg\max_{j: j \sim i} \cos(\widetilde{\mathbf{\Pi}}_i, \mathbb{I}_j).$$

Intuitively,  $\beta_i$  measures how  $\mathbf{\Pi}_i$  is distinguishable from a one-to-one mapping, which is estimated by the distance between the largest element in  $\widetilde{\mathbf{\Pi}}_i$  (length-normalized) and one within group. We can see that  $\beta_i = 0$  if  $\mathbf{\Pi}_i = \mathbb{I}_j$  for some  $j \sim i$ , and  $\beta_i \neq 0$  when  $\mathbf{\Pi}_i$  represents a one-to-many mapping. Thus, the support  $\mathcal{C} = \{i \in [n] : \beta_i \neq 0\}$  indexes the rows where  $\mathbf{\Pi}_i$  corresponds to one-to-many mapping. To recover the support  $\mathcal{C}$  and construct a sparse estimate of  $\mathbf{\Pi}$ , denoted as  $\widehat{\mathbf{\Pi}}^{[2]}$ , we threshold  $\widetilde{\beta}_i$  with a properly chosen  $\lambda_n$  and obtain the  $i^{\text{th}}$  row of  $\widehat{\mathbf{\Pi}}^{[2]}$  as

$$\widehat{\mathbf{\Pi}}_i^{[2]} = \mathbb{I}_{\widetilde{j}_i} \mathbb{1}(\widetilde{\beta}_i \leq \lambda_n) + \frac{\widetilde{\mathbf{\Pi}}_i}{\|(\widetilde{\mathbf{\Pi}}_i, \mathbb{X})^\top\|_2} \mathbb{1}(\widetilde{\beta}_i > \lambda_n) \quad (6)$$

where we suppressed  $\lambda_n$  in  $\widehat{\mathbf{\Pi}}^{[2]}$  for ease of notation. Thus, we set  $\widehat{\mathbf{\Pi}}_i^{[2]}$  to  $\mathbb{I}_{\widetilde{j}_i}$  when  $\widetilde{\beta}_i$  is small; but estimate  $\mathbf{\Pi}_i$  as  $\widetilde{\mathbf{\Pi}}_i / \|(\widetilde{\mathbf{\Pi}}_i, \mathbb{X})^\top\|_2$  when  $\widetilde{\beta}_i$  is large. The  $\ell_2$ -normalized estimator  $\widetilde{\mathbf{\Pi}}_i / \|(\widetilde{\mathbf{\Pi}}_i, \mathbb{X})^\top\|_2$  preserves unit length for the translated vector  $(\widetilde{\mathbf{\Pi}}_i, \mathbb{X})^\top$  and in fact is the solution to minimizing the constrained OLS problem under the spherical constraint.

With a properly chosen  $\lambda_n$ ,  $\widehat{\mathbf{\Pi}}^{[2]}$  consistently recovers  $\mathbf{\Pi}$  as detailed in Section 3.2. Intuitively, to correctly classify  $\mathbf{\Pi}_i$  as a one-to-one or one-to-many mapping,  $\lambda_n$  should be chosen to be both below the smallest non-zero signal of  $\beta_i$  and above the estimation error for the zero-signals. In practice,  $\lambda_n$  is selected among a series of values in  $(0, 1 - \frac{1}{\sqrt{2}})$  by cross-validation, where the upper bound was chosen because there is at most one  $j$  that gives  $\cos(\widetilde{\mathbf{\Pi}}_i, \mathbb{I}_j) > \frac{1}{\sqrt{2}}$ . Specifically, we use cross-validation optimizing the mean squared

error for prediction of  $\mathbb{Y}$ , defined as  $\sum_{cv} \|\mathbb{Y}_{cv} - \widehat{\Pi}^{[2]} \mathbb{X}_{cv} \widehat{\mathbb{W}}\|_F^2$ , where  $\mathbb{Y}_{cv}$  and  $\mathbb{X}_{cv}$  denote the combination of selected columns of  $\mathbb{Y}$  and  $\mathbb{X}$ , respectively, which serve as validation data.

In step III, based on the updated mapping estimate  $\widehat{\Pi}^{[2]}$ , we obtain a refined estimator for  $\mathbb{W}$  using the subsample that we estimate to be correctly matched as

$$\widehat{\mathbb{W}}^{[2]} = \mathcal{U} \left( \mathbb{X}_{[\mathcal{S}(\widehat{\Pi}^{[2]})],:}^\top \mathbb{Y}_{[\mathcal{S}(\widehat{\Pi}^{[2]})],:} \right), \quad \text{where } \mathcal{S}(\widehat{\Pi}^{[2]}) = \{i \in [n] : \widehat{\Pi}_i^{[2]} = \mathbb{I}_i\}.$$

### 3 Theoretical Properties of the iSphereMAP Estimators

#### 3.1 Properties of the initial translation matrix estimator $\widehat{\mathbb{W}}^{[1]}$

We first investigate whether  $\widehat{\mathbb{W}}^{[1]}$  from the initial spherical regression (2) can consistently estimate  $\mathbb{W}$  despite the presence of mismatch in the data. Intuitively, if only a small fraction of the data is mismatched, the distortion in  $\widehat{\mathbb{W}}^{[1]}$  due to mismatch may be negligible. The following theorem presents the error bound of  $\widehat{\mathbb{W}}^{[1]}$ , which is proved in Section B.1 of the supplementary material.

**Theorem 1.** *For any  $t > 0$ , if  $\gamma_{\kappa,p} \sigma_p(\mathbb{X})^2 > t \sqrt{n(1 - \gamma_{\kappa,p}^2)} + 2\gamma_{\kappa,p} n_{\text{mis}}$ , then with probability at least  $1 - 1/t^2$ ,*

$$\|\widehat{\mathbb{W}}^{[1]} - \mathbb{W}\|_F \leq \frac{t \sqrt{n(1 - \gamma_{\kappa,p}^2)} + 2\gamma_{\kappa,p} n_{\text{mis}}}{\gamma_{\kappa,p} \sigma_p(\mathbb{X})^2 - t \sqrt{n(1 - \gamma_{\kappa,p}^2)} - 2\gamma_{\kappa,p} n_{\text{mis}}}. \quad (7)$$

**Remark 1.** *The quantity  $\sigma_p(\mathbb{X})$  describes the colinearity of columns of  $\mathbb{X}$ , with a larger value suggesting less linearly dependent rows. If  $p > n$ ,  $\sigma_p(\mathbb{X}) = 0$ . When  $n \geq p$  and rows of  $\mathbb{X}$  are stochastically generated with a uniform distribution over the surface of the hypersphere  $\mathcal{S}^{p-1}$ ,  $\sigma_p(\mathbb{X})$  is roughly of the order  $O(\sqrt{n/p})$  as  $n$  and  $p$  grow. This rate decreases as  $p$  increases, mainly because of the spherical assumption that rows of  $\mathbb{X}$  are of unit length.*

**Remark 2.** *The error bound in Theorem 1 also depends on the scaling factor  $\gamma_{\kappa,p} \in (0, 1)$*

introduced in Section 2.2.1. In fact, the term

$$\eta_{\kappa,p} \equiv 1 - \gamma_{\kappa,p}^2$$

describes the inherent noise in the data, with  $E[\|\mathbb{X}^\top(\mathbb{Y} - E[\mathbb{Y}])\|_F^2] = n(1 - \gamma_{\kappa,p}^2)$  and  $E[(\mathbb{Y} - E[\mathbb{Y}])((\mathbb{Y} - E[\mathbb{Y}])^\top)] = (1 - \gamma_{\kappa,p}^2)\mathbb{I}_n$ . The noise level  $\eta_{\kappa,p}$ , determined by the order of  $p$  and  $\kappa$ , drives the precision of the iSphereMAP estimators. In particular, if  $p$  and  $\kappa$  are fixed, then  $\eta_{\kappa,p}$  is a positive constant with  $\eta_{\kappa,p} \in (0, 1)$ . The larger  $\kappa$  is, the more concentrated the data is around  $\boldsymbol{\mu}$ , the closer  $\eta_{\kappa,p}$  is to 0. If  $p/\kappa = o(1)$  and  $p \geq 4$ , then  $\eta_{\kappa,p} \rightarrow 0$  as  $\kappa \rightarrow \infty$  by Lemma 1. One can interpret the two scenarios of  $p$  and  $\kappa$  as noisy and approximately noiseless in analogy to the Gaussian setting.

The following corollary simplifies the error bound of  $\widehat{\mathbb{W}}^{[1]}$  in the scenarios when  $\eta_{\kappa,p}$  is a fixed constant or goes to zero as discussed in Remark 2, which is proved in Section B.2 of the supplementary material. The conditions required to achieve consistency is weaker than that in Chang (1986).

**Corollary 1.** Suppose  $\gamma_{\kappa,p} > \rho$  for some constant  $\rho \in (0, 1)$  that does not depend on  $\kappa$  and  $p$ ,  $n \rightarrow \infty$ , and  $n_{\text{mis}} = o(\sigma_p(\mathbb{X})^2)$ . Then we have

$$\|\widehat{\mathbb{W}}^{[1]} - \mathbb{W}\|_F = \begin{cases} O_P\left(\frac{\sqrt{n} + n_{\text{mis}}}{\sigma_p(\mathbb{X})^2}\right) & \text{if } p \text{ and } \kappa \text{ are fixed, } \sqrt{n} = o(\sigma_p(\mathbb{X})^2) \\ O_P\left(\frac{\sqrt{n\eta_{\kappa,p}} + n_{\text{mis}}}{\sigma_p(\mathbb{X})^2}\right) & \text{if } \sqrt{n\eta_{\kappa,p}} = o(\sigma_p(\mathbb{X})^2). \end{cases} \quad (8)$$

In particular,  $\|\widehat{\mathbb{W}}^{[1]} - \mathbb{W}\|_F$  converges to 0 in probability in both cases.

**Remark 3.** When  $p/\kappa = o(1)$ ,  $\kappa \rightarrow \infty$ ,  $p \geq 4$ , we have that  $\eta_{\kappa,p} = O(p/\kappa)$ . In this case  $\sqrt{n\eta_{\kappa,p}} = o(\sigma_p(\mathbb{X})^2)$  if  $\sqrt{np/\kappa} = o(\sigma_p(\mathbb{X})^2)$ . Thus we can consistently recover  $\mathbb{W}$  as long as the rate at which  $\sigma_p(\mathbb{X})$  grows is faster than both  $n_{\text{mis}}$  and  $\sqrt{np/\kappa}$ . In addition, note that  $\sigma_p(\mathbb{X}) \leq \|\mathbb{X}\|_F = \sqrt{n}$ . Therefore  $n_{\text{mis}} = o(\sigma_p(\mathbb{X})^2)$  indicates  $n_{\text{mis}} = o(n)$ .

**Remark 4.** Assuming  $\sigma_p(\mathbb{X}) = O(\sqrt{n/p})$  as described in Remark 1, we can see from Corollary 1 that as  $n \rightarrow \infty$ ,  $\|\widehat{\mathbb{W}}^{[1]} - \mathbb{W}\|_F = o_P(1)$  under either of the following asymptotic regimes: (1)  $p$  and  $\kappa$  are fixed and  $n_{\text{mis}} = o(n)$ ; or (2)  $\kappa \rightarrow \infty$ ,  $p \geq 4$ ,  $p = o(\kappa)$ ,  $n_{\text{mis}} = o(n/p)$  and  $p^3 = o(n\kappa)$ .

### 3.2 Properties of the Mapping Matrix estimator

Since the mapping matrix estimator  $\widehat{\mathbf{\Pi}}^{[2]}$  is a thresholded version of the initial OLS estimator  $\widetilde{\mathbf{\Pi}} = \text{diag}\{\widetilde{\mathbf{\Pi}}^1, \dots, \widetilde{\mathbf{\Pi}}^K\}$ , we first establish the convergence rate for  $\widetilde{\mathbf{\Pi}}^k$  in the following theorem.

**Theorem 2.** *If  $n \rightarrow \infty$ ,  $p \geq 4$ ,  $n > p > \max_{1 \leq k \leq K} n_k$ ,  $\gamma_{\kappa, p} > \rho$  for some constant  $\rho \in (0, 1)$  that does not depend on  $\kappa$  and  $p$ ,  $\sqrt{n\eta_{\kappa, p}} = o(\sigma_p(\mathbb{X})^2)$ , and  $n_{\text{mis}} = o(\sigma_p(\mathbb{X})^2)$ , then*

$$\|\widetilde{\mathbf{\Pi}}^k - \mathbf{\Pi}^k\|_F = O_p \left( \sigma_{n_k}(\mathbb{X}_{[G_k, :]})^{-1} \sqrt{n_k} \left\{ \sqrt{\frac{p}{\kappa}} + \frac{\sqrt{n\eta_{\kappa, p}} + n_{\text{mis}}}{\sigma_p(\mathbb{X})^2} \right\} \right), \quad (9)$$

for  $k = 1, \dots, K$ . In addition, assume that  $K \rightarrow \infty$  and  $4 \log K \leq p \min_{1 \leq k \leq K} n_k$ . Then,

$$\max_{1 \leq k \leq K} \|\widetilde{\mathbf{\Pi}}^k - \mathbf{\Pi}^k\|_F = O_p \left( \left[ \min_{1 \leq k \leq K} \sigma_{n_k}(\mathbb{X}_{[G_k, :]}) \right]^{-1} \max_{1 \leq k \leq K} \sqrt{n_k} \left\{ \sqrt{\frac{p}{\kappa}} + \frac{\sqrt{n\eta_{\kappa, p}} + n_{\text{mis}}}{\sigma_p(\mathbb{X})^2} \right\} \right). \quad (10)$$

**Remark 5.** *The term  $\min_{1 \leq k \leq K} \sigma_{n_k}(\mathbb{X}_{[G_k, :]})$  indicates the within group variation of the design matrix rows. In particular, if we assume that the pairwise cosine similarity within each group is no greater than  $a$  where  $a \leq \frac{1}{\max n_k - 1}$ , then  $\min_{1 \leq k \leq K} \sigma_{n_k}(\mathbb{X}_{[G_k, :]}) \geq 1 - (\max n_k - 1)a$ .*

**Remark 6.** *If the number of groups  $K$  is fixed, then derivation from (9) to (10) is trivial. Our result concerns the nontrivial scenario when  $K \rightarrow \infty$ , in which case proof of Equation (10) requires specific analysis of the tail bound behavior of the vMF distribution detailed in Proposition A.1 of the supplementary material.*

**Remark 7.** *We discuss the asymptotic regime required by Theorem 2 for the case where all groups have equal group size with  $n_k \equiv n/K$ ,  $\kappa \rightarrow \infty$ ,  $p \geq 4$ ,  $p = o(\kappa)$ , and  $\sigma_p(\mathbb{X})$  is of the order  $\sqrt{n/p}$  as described by Remark 1. First,  $p$  needs to be small enough compared to  $n$ ,  $\kappa$  and  $n\kappa$  ( $p = o(\kappa)$  and  $p = o(n^{1/3}\kappa^{1/3})$  by Remark 4, and  $p < n$ ) so that the error rate of  $\widehat{\mathbb{W}}^{[1]}$  is controlled by Corollary 1. Second,  $p$  needs to be larger than  $n_k \equiv n/K$  so that the OLS has a unique solution. Third, the mismatch needs to be sparse enough such that  $n_{\text{mis}} = o(n/p)$  by Remark 4. In summary, suppose  $p = n^\alpha$ ,  $\kappa = n^\beta$ , and  $K = n^\gamma$ , then the conditions of Theorem 2 are satisfied when  $0 < \gamma < 1$ ,  $1 - \gamma < \alpha < \min(1, (1 + \beta)/3, \beta)$ , and  $n_{\text{mis}} = o(n^{1-\alpha})$ .*

Interpretation of Theorem 2 is relatively straightforward. The origin of the error in the initial OLS estimate of  $\mathbf{\Pi}^k$  is four-fold. First, the inherent error of the vMF distribution

contributes the term  $\sqrt{p/\kappa}$ . This is a unique tail bound property of the vMF distribution which we derive in Proposition A.1 of the supplementary materials. In particular, when  $p$  is fixed, or  $p = o(\kappa)$ , then as the concentration parameter  $\kappa$  goes to infinity, the data approaches the noiseless situation and this term goes to zero. Second, by Corollary 1, the estimation error of  $\mathbb{W}$  in the previous step contributes the term  $\sigma_p(\mathbb{X})^{-2}(\sqrt{n\eta_{\kappa,p}} + n_{\text{mis}})$ . Third, the error bound of  $\tilde{\Pi}^k$  is proportionally dependent on the size of  $\Pi^k$ . Lastly, if two rows within the same group have cosine similarity approaching one, then they are indistinguishable. Accordingly, the error bound is also scaled by the separability of rows in the design matrix  $\mathbb{X}_{[G_k, :]}$  as discussed in *Remark 5*. The proof of Theorem 2 can be found in Section B.3 of the supplementary materials.

With the additional thresholding step,  $\hat{\Pi}^{[2]}$  attains model selection consistency as summarized in the following theorem, which is proved in Section B.4 of the supplementary materials.

**Theorem 3.** *Suppose that the assumptions in Theorem 2 hold. Let  $\mathcal{B}_{\min} = \min_{i \in \mathcal{C}} \beta_i$  and*

$$c_n = \left[ \min_{1 \leq k \leq K} \sigma_{n_k}(\mathbb{X}_{[G_k, :]}) \right]^{-1} \max_{1 \leq k \leq K} \sqrt{n_k} \left\{ \sqrt{\frac{p}{\kappa}} + \sigma_p(\mathbb{X})^{-2}(\sqrt{n\eta_{\kappa,p}} + n_{\text{mis}}) \right\}.$$

*We further assume that  $c_n \max_{1 \leq k \leq K} \sqrt{n_k} \ll \mathcal{B}_{\min}^2$ , and  $c_n \max_{i \in \mathcal{C}} \|\Pi_i\|_2 \max_{1 \leq k \leq K} \sqrt{n_k} \rightarrow 0$ . Then, for  $c_n \ll \lambda_n \ll \mathcal{B}_{\min}$ , as  $n \rightarrow \infty$ , the following holds with probability approaching one*

$$\begin{aligned} & \text{for all } i \in \mathcal{C}, \max_{i \in \mathcal{C}} \|\hat{\Pi}_i^{[2]} - \Pi_i\|_2 \rightarrow 0 \\ & \text{for all } i \notin \mathcal{C}, \hat{\Pi}_i^{[2]} = \Pi_i = \mathbb{I}_{j..} \end{aligned} \tag{11}$$

Theorem 3 states that, as  $n$  increases, our hard-thresholding procedure can distinguish between one-to-one and one-to-many mapping, correctly locate the matched row for one-to-one mapping, and consistently estimate the weight vector for one-to-many mapping.

**Remark 8.** *The model selection consistency in Theorem 3 requires  $p/\kappa = o(1)$ , under which the noise level  $\eta_{\kappa,p} = E[\|\mathbf{Y}_i - E[\mathbf{Y}_i]\|_2^2] = o(1)$ . Although not directly comparable, a similar condition was required in Pananjady et al. (2016) where they assumed the following univariate linear regression  $\mathbf{Y} = \Pi \mathbb{X} \mathbf{w} + \mathbf{U}$ , with  $\Pi$  being a permutation matrix and  $\mathbf{X}$  being*

*Gaussian. They studied the maximum likelihood estimate of  $\mathbf{\Pi}$  with the restriction of  $\mathbf{\Pi}$  being a permutation matrix. They showed that exact permutation recovery requires that the signal-to-noise ratio goes to infinity at a polynomial order of  $n$ . We require the noise level  $\eta_{\kappa,p} = o(1)$  but do not require a specific rate.*

**Remark 9.** *To provide some intuition for the choice of  $\lambda_n$ , we note that if  $i \in \mathcal{C}$ , i.e., the true  $\mathbf{\Pi}_i$  in fact represents a one-to-many mapping, then  $\beta_i \neq 0$ . Thus  $\lambda_n$  should be chosen to be much smaller than the smallest non-zero signal  $\mathcal{B}_{\min}$ . On the other hand, if  $i \notin \mathcal{C}$ , then  $\beta_i = 0$  and  $\lambda_n$  should be able to tolerate the error in the initial estimate  $\tilde{\mathbf{\Pi}}$  and correctly threshold  $\tilde{\beta}_i$  to zero. The lower bound  $c_n$  represents the order of  $\max_{1 \leq k \leq K} \|\tilde{\mathbf{\Pi}}^k - \mathbf{\Pi}^k\|_F$  by Theorem 2. By letting  $\lambda_n \gg c_n$ , we would successfully set the corresponding  $\tilde{\beta}_i$  to zero.*

### 3.3 Properties of the Refined translation matrix estimator $\widehat{\mathbb{W}}^{[2]}$

From Corollary 1, the error bound of the initial estimate  $\widehat{\mathbb{W}}^{[1]} = \mathcal{U}(\mathbb{X}^\top \mathbb{Y})$  consists of two terms of order  $\sigma_p(\mathbb{X})^{-2} n_{\text{mis}}$  and  $\sigma_p(\mathbb{X})^{-2} \sqrt{n \eta_{\kappa,p}}$  respectively, with the first term accounting for the mismatch error. If  $\widehat{\mathbf{\Pi}}^{[2]}$  accurately identifies the mismatch patterns, then one would expect  $\widehat{\mathbb{W}}^{[2]}$  to have lower error due to the removal of the mismatched pairs from estimating  $\widehat{\mathbb{W}}^{[2]}$ . The following corollary summarizes the error rate of  $\widehat{\mathbb{W}}^{[2]}$ , which is proved in Section B.5 of the supplementary materials.

**Corollary 2.** *Under the assumptions of Theorems 2 and 3, as  $n \rightarrow \infty$  we have*

$$\|\widehat{\mathbb{W}}^{[2]} - \mathbb{W}\|_F = O_P \left( \frac{\sqrt{(n - n_{\text{mis}}) \eta_{\kappa,p}}}{\sigma_p(\mathbb{X}_{[\mathcal{S}(\mathbf{\Pi}),:]})^2} \right) = O_P \left( \frac{\sqrt{n \eta_{\kappa,p}}}{\sigma_p(\mathbb{X})^2} \right). \quad (12)$$

**Remark 10.** *We observe that  $n - n_{\text{mis}}$  is of the same order as  $n$  because  $n_{\text{mis}} = o(n)$  is a necessary condition as discussed in Remark 4. In addition,  $\sigma_p(\mathbb{X}_{[\mathcal{S}(\mathbf{\Pi}),:]})^2$  and  $\sigma_p(\mathbb{X})^2$  are of the same order when  $n_{\text{mis}} = o(\sigma_p(\mathbb{X})^2)$ , which is shown in Section B.5 of the supplementary materials.*

Corollary 2 indicates that estimating  $\mathbb{W}$  using only pairs deemed as matched by  $\widehat{\mathbf{\Pi}}^{[2]}$  reduces the error due to mismatch at the cost of reduced sample size  $n - n_{\text{mis}}$ . However, since  $n_{\text{mis}} = o(n)$ ,  $\widehat{\mathbb{W}}^{[2]}$  attains the same error rate as the estimator obtained with  $\mathbf{\Pi}$  given or

$\mathbf{\Pi} = \mathbb{I}$ . That is, the iSphereMAP estimator  $\widehat{\mathbb{W}}^{[2]}$  achieves an error rate that is as good as if no mismatch is present. Moreover, compared to the error rate of  $O_P\{(\sqrt{n\eta_{\kappa,p}} + n_{\text{mis}})/\sigma_p(\mathbb{X})^2\}$  in (8),  $\widehat{\mathbb{W}}^{[2]}$  attains a lower error rate than that of  $\widehat{\mathbb{W}}^{[1]}$  when  $\sqrt{n\eta_{\kappa,p}} = o(n_{\text{mis}})$ .

## 4 Simulation

We have conducted extensive simulation studies to evaluate the performance of our proposed iSphereMAP method for estimating both  $\mathbb{W}$  and  $\mathbf{\Pi}$  and to compare to the Mikolov et al. (2013) approach, referred to as the MT method hereafter. Specifically, for each  $i$ , the MT method finds  $j_i = \arg \max_j \cos(\mathbf{Y}_i, \widehat{\mathbb{W}}\mathbf{X}_j)$  without using group information, where  $\widehat{\mathbb{W}}$  is estimated by the OLS. We compare (1)  $\mathbb{W}$  estimated from our proposed spherical regression and from OLS using full data and refined data; (2)  $\mathbf{\Pi}$  estimated from our hard-thresholding procedure using group information, and from the MT method without group information.

Throughout our simulation, we set  $p = \kappa = 300$ , and all results are averaged over 100 simulation datasets. This is a scenario where the noise level is relatively higher than the theoretical settings. We also investigate the setting with a low noise level compatible with the theoretical settings in Section D of the supplementary material. For a given sample size  $n$ , we let the true mapping matrix  $\mathbf{\Pi}$  include  $n_{\text{mis}} = n^\alpha$  mismatched rows. We considered fixing  $n = 8000$  with  $\alpha$  ranging from 0.35 to 0.93, corresponding to 0.3% to 53% of mismatched pairs among the entire data. We also considered fixing  $\alpha = 0.8$  but with  $n$  varying from approximately 2000 to 8000. The sample size  $n$  increases as the number of groups  $K$  increases. Specifically, we prespecify a list of 1700 unequal group sizes. We select the first  $K$  group sizes in the list, with  $K$  ranging from 100 to 1700, such that  $n$  increases from approximately 2000 to 8000. In each setting with a specific set of  $(K, n, \alpha)$ , we first simulate  $\mathbb{X}$  by generating  $n$  vectors that follow mixture of  $K$  vMF distributions with concentration parameter  $\kappa$ , whose mean directions are  $K$  group centers uniformly distributed on  $\mathcal{S}^{p-1}$ . The mixture weight for the distribution of the corresponding group is twice the weight for the other  $K - 1$  distributions. Then we generate  $\mathbf{\Pi} = \text{diag}\{\mathbf{\Pi}^1, \dots, \mathbf{\Pi}^K\}$ , in which randomly selected  $n - n^\alpha$  rows are copied from the corresponding rows of  $\mathbb{I}_n$ , whereas the other  $n^\alpha$  rows are specified to encode one-to-one and one-to-many mismatch patterns. We let half of the  $n^\alpha$  rows be indicators that introduce permutation within group and the other half be

weight vectors following the Uniform(0,1) distribution to introduce one-to-many mapping. We specify the true transformation matrix  $\mathbb{W}$  by taking the left eigenvectors of a  $p \times p$  matrix of standard normal random values. Finally, we generate  $\mathbb{Y}$  with mean directions  $\mathbf{\Pi}\mathbb{X}\mathbb{W}$  following the vMF distribution with concentration parameter  $\kappa$ .

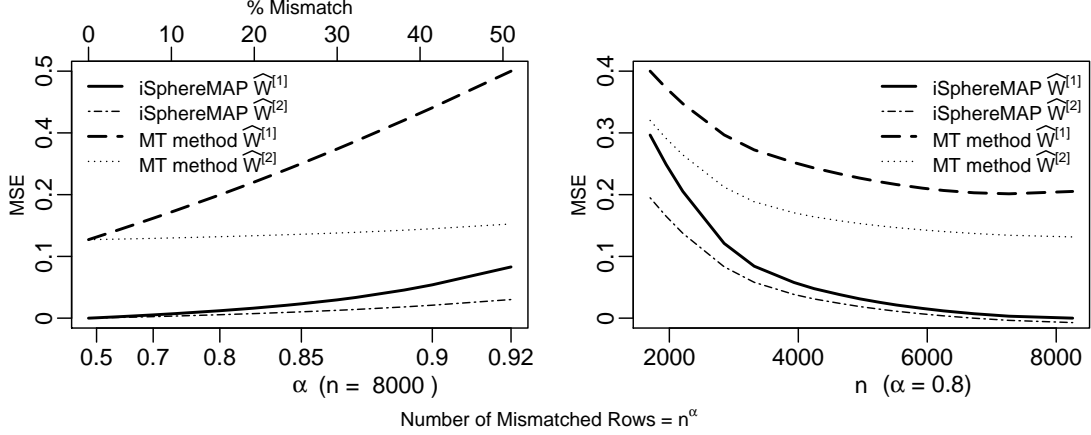


Figure 1: Performance of  $\hat{\mathbb{W}}^{[1]}$  and  $\hat{\mathbb{W}}^{[2]}$  obtained based on the proposed spherical regression and OLS in terms of the MSE (normalized by  $p^{-1} = 1/300$ ) under ranging amount of mismatch (left panel) and sample size (right panel).

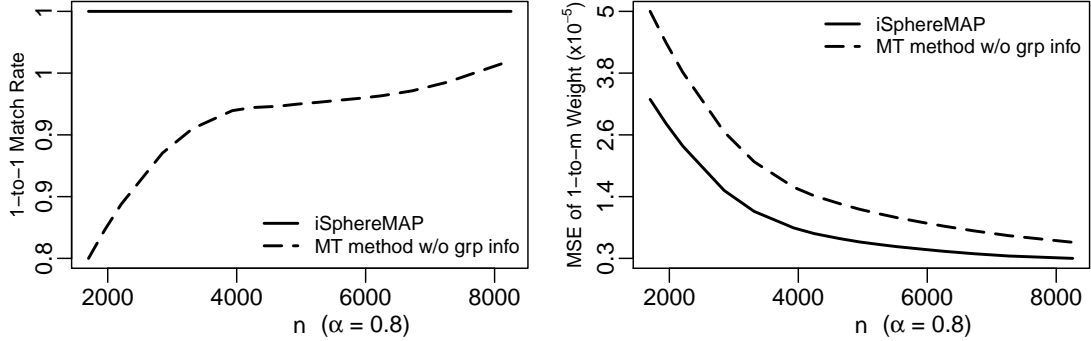


Figure 2: Performance of  $\hat{\mathbf{\Pi}}^{[2]}$  estimated with and without group information in terms of the one-to-one match rate (left panel) and the MSE of one-to-many weight (right panel).

We first summarize in Figure 1 the mean squared errors (MSEs) scaled by  $p^{-1}$  of  $\hat{\mathbb{W}}^{[1]}$  and  $\hat{\mathbb{W}}^{[2]}$  from spherical regression and the MT method (OLS). The MSE is defined as the average of  $\|\hat{\mathbb{W}} - \mathbb{W}\|_F^2$  over simulated datasets. The spherical regression attained considerably smaller estimation error compared to the MT method in both  $\hat{\mathbb{W}}^{[1]}$  and  $\hat{\mathbb{W}}^{[2]}$ . As  $\alpha$



and correspondingly  $n_{\text{mis}}$  increases, both methods suffer increased error as expected but the deterioration is much more drastic for the OLS. For a fixed  $\alpha = 0.8$ , the estimation error of spherical regression approaches to 0 in a much faster rate than that of the OLS as  $n$  increases.

By removing the unmatched pairs, substantial improvement is observed in  $\widehat{\mathbb{W}}^{[2]}$  compared to  $\widehat{\mathbb{W}}^{[1]}$ . In particular, when  $n_{\text{mis}} = n^\alpha$  ranged from  $n^{0.7}$  to  $n^{0.93}$ , the MSEs from both methods are notably smaller than that of the initial estimates. Our observation is consistent with our discussion in Section 3.3 that when the order of  $n_{\text{mis}}$  is larger than  $\sqrt{n\eta_{\kappa,p}} = n^{0.5}$ , the error rate of the refined estimate will be improved. When  $\alpha$  is fixed at 0.8,  $\widehat{\mathbb{W}}^{[2]}$  still have a consistently smaller MSE than  $\widehat{\mathbb{W}}^{[1]}$ , with the difference in MSE between  $\widehat{\mathbb{W}}^{[1]}$  and  $\widehat{\mathbb{W}}^{[2]}$  from spherical regression decreasing as  $n$  increases.

We next evaluate the performance of  $\widehat{\Pi}^{[2]}$  estimated using data  $(\widehat{\mathbb{W}}^{[1]}\mathbb{X}, \mathbb{Y})$  with and without the aid of group information, where  $\widehat{\mathbb{W}}^{[1]}$  is obtained from spherical regression. Note that without a group structure, initial OLS estimate  $\widetilde{\Pi}$  may not be obtained due to the high dimensionality. In this case, we estimate a permutation matrix using the MT method which matches rows of  $\widehat{\mathbb{W}}^{[1]}\mathbb{X}$  and  $\mathbb{Y}$  using cosine similarity as distance metric. We evaluate both the one-to-one match rate and the MSE of one-to-many weight defined as follows. The one-to-one match rate is the percentage of correctly matched rows among all one-to-one mappings. Specifically, we calculate the one-to-one match rate as  $|\{i : \widehat{\Pi}_i = \Pi_i, i \in \mathcal{C}^c\}|/|\mathcal{C}^c|$ , where  $\mathcal{C}^c$  is the complement of  $\mathcal{C}$ , i.e., the true index set of one-to-one mapping. The MSE of one-to-many weight is defined as the MSE of  $\widehat{\Pi}_{[\mathcal{C},:]}$  normalized by its size  $|\mathcal{C}|n$ . We also access the percentage of correctly identified one-to-many mappings, i.e.,  $|\widehat{\mathcal{C}} \cap \mathcal{C}|/|\mathcal{C}|$ , where  $\widehat{\mathcal{C}}$  denotes the estimated set of one-to-many mapping.

Figure 2 presents the performance of  $\widehat{\Pi}$  estimated from our method with group information and from the MT method without group information, with a goal to understand the amount of accuracy gain from the group information. As  $n$  increases, the match rate for one-to-one mapping increases and the MSE of the weight vectors decreases. Our proposed method using group information outperforms the MT method without group structure in terms of both the one-to-one match rate and the MSE of one-to-many mapping weight. Moreover, our proposed hard-thresholding procedure can correctly identify 95% of the one-to-many mappings on average across all scenarios, whereas the MT method does not allow

for one-to-many mapping.

## 5 Application: ICD code Translation

In this section, we propose to employ the iSphereMAP method to (i) map the ICD-9 codes between two healthcare systems, the Partners HealthCare System (PHS) and the Veterans Health Administration (VHA); and (ii) to automatically translate between ICD-9 and ICD-10 codes using VHA data. For the between healthcare ICD mapping, we focused on the ICD-9 codes only since the majority of the codes recorded in the EHR are ICD-9 codes. In both examples, we use the `word2vec` algorithm to obtain  $p = 300$  dimensional SEVs for all relevant ICD codes. The algorithm essentially learns the interpretation of the ICD codes in clinical practice from the co-occurrence patterns of codes in the EHRs as detailed in Beam et al. (2018). The code SEVs are  $\ell_2$ -normalized within the healthcare system to represent  $\mathbb{X}$  and  $\mathbb{Y}$  respectively.

### 5.1 Mapping ICD-9 codes between VHA and PHS

There are a total of  $n = 8823$  ICD-9 code SEVs from the two healthcare systems available for analysis. Grouping information on the ICD codes is available through the ICD hierarchy (World Health Organization 1977, Centers for Disease Control and Prevention 2015), the Clinical Classification Software (Agency for Healthcare Research and Quality 2012), or the ICD-to-phenotype mapping provided by the phenome-wide association study (PheWAS) catalogue Denny et al. (2010). We chose the PheWAS code (namely phecode) as it represents clinically meaningful phenotypes. Due to the hierarchical nature of the phecodes, we collapsed all phecodes with the same integer values into the same group, resulting in  $K = 578$  groups. The ICD-9 codes from different phecode groups represent distinct phenotypes and thus are unlikely to be confused with each other. As such, no mismatch is expected to occur across phecode groups. On the other hand, we expect to see mismatch within phecode groups. It has been shown that for a specific disease or procedure, the level of agreement among coders and agencies in assigning medical codes can be poor (Austin et al. 2002, O’malley et al. 2005), in part due to the fact that multiple codes can be appropriate for describing the same diagnosis.

Figure 3 presents the first three principal components of ICD-9 codes belonging to four select phecode-groups from VHA and PHS. Each point represents an ICD-9 code color-coded by the phecode-group it belongs to. First of all, the code-vectors in VHA and PHS generally show distinct patterns, reflecting the variation in languages used in the two healthcare systems that necessitates alignment of the two language spaces. Second, although the codes are clustered by the phecode-group, many of the groups are distributed on top of each other, suggesting the difficulty in matching the codes without prior group information.

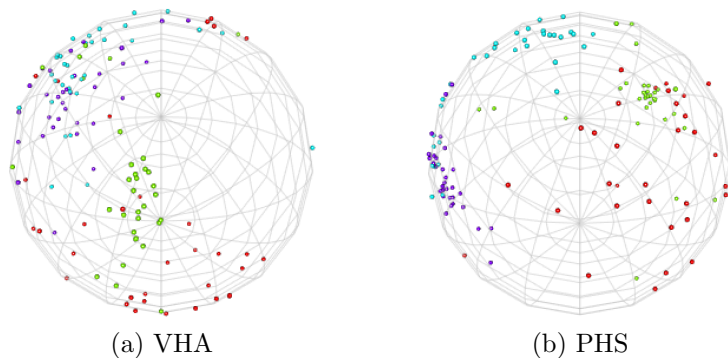


Figure 3: First three principal components of ICD-9 code vectors in four select phecode groups from Veterans Health Administration (left) and Partners HealthCare Systems (right). Each point represents an ICD-9 code, and is color-coded by the phecode-grouping.

We select two groups of ICD-9 codes to present the result: one describing symptoms of respiratory system, the other describing pain in joint. Figure 4 presents the estimated mapping of codes from VHA (left) to PHS (right) from the iSphereMAP procedure. Thicker lines indicate larger weight for the corresponding codes on the right, and we did not link codes with negative weights. In Figure 4 (a), ICD-9 code 786.09 describing “Other dyspnea and respiratory abnormality” was mapped to multiple codes with higher weights on both itself and code 786.05 describing “shortness of breath”, which is semantically similar to “dyspnea”. These two codes are likely to be used in an exchangeable manner. In Figure 4 (b), most codes have a one-to-one correspondence. However, codes 719.40 and 719.48 in VHA were mapped to multiple codes in PHS. Both codes describe joint pain with unspecified sites. It is thus reasonable to interpret these codes by combinations of codes associated with different specific sites or unspecified sites.

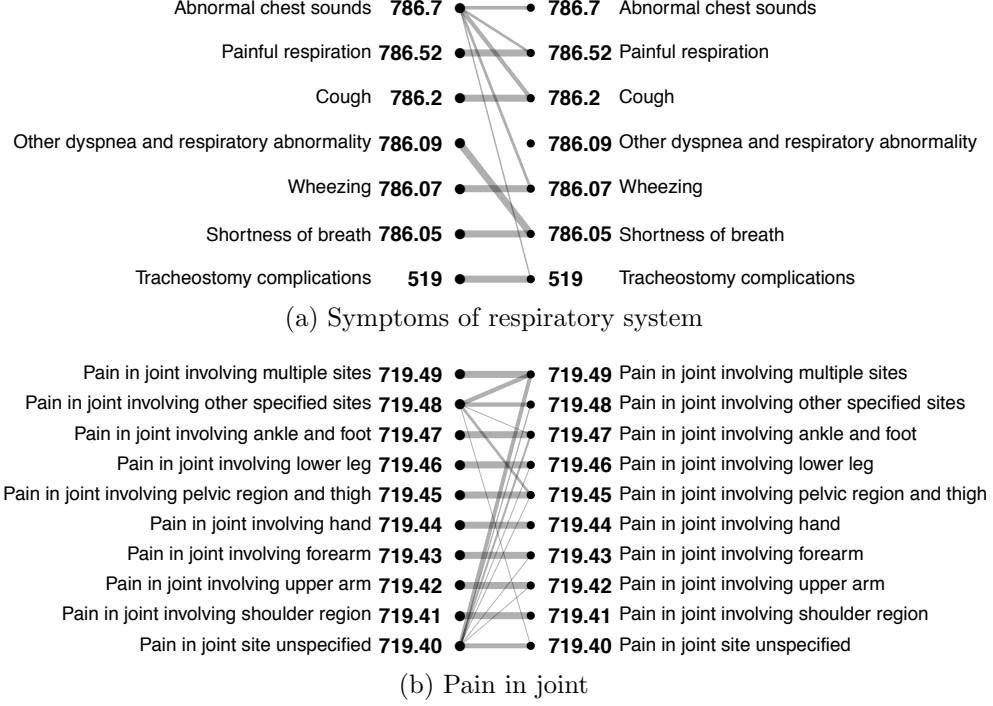
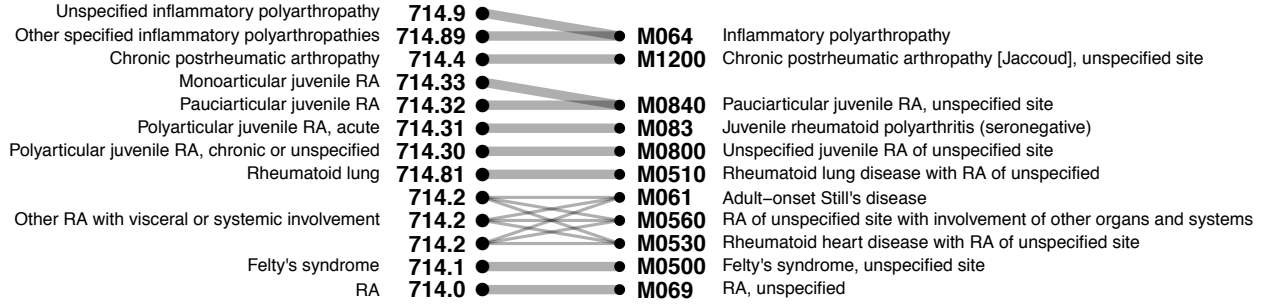


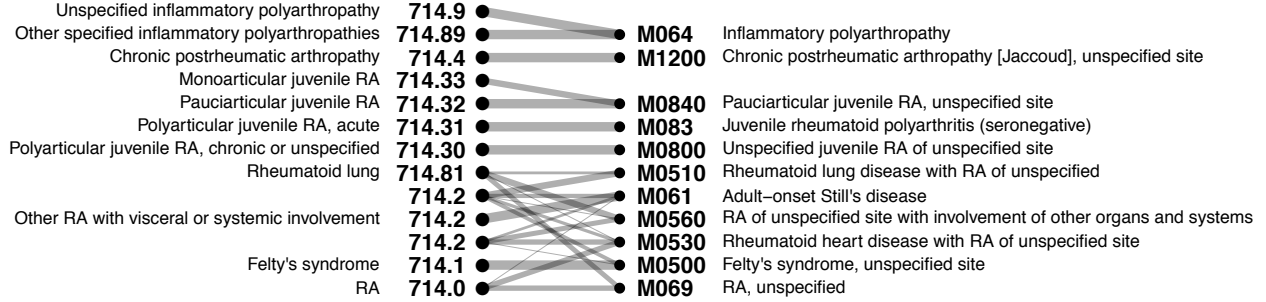
Figure 4: Plot of the estimated mapping of codes from VHA (left) to PHS (right). Selected codes belong to the group describing (a) symptoms of respiratory system, and (b) pain in joint. Thicker line indicates larger weight on the corresponding codes on the right.

## 5.2 Translation between ICD-9 and ICD-10 codes

We also applied our method to automatically map between ICD-9 and ICD-10 codes using VHA data. We train ICD-9 and ICD-10 code-vectors using data from non-overlapping time period, thus each set of vectors forms a language space. We take the GEM mapping available through the CMS (Roth 2016) as a benchmark. As discussed in Section 1.1, due to the complexity and large number of ICD-10 codes, many mappings are one-to-many or approximate match in GEM. For example, Figure 5 (a) displays the GEM mapping for ICD-9 codes in the rheumatoid arthritis (RA) group, which includes one-to-one, one-to-many, and many-to-one mappings and all are marked as “approximate”. When an ICD-9 code should map to the combination of the corresponding ICD-10 codes according to the GEM mapping, e.g. “714.2” in Figure 5 (a), we duplicate the ICD-9 code vector rows to match the number of ICD-10 codes to introduce mismatch error in the data  $\mathbb{X}$  and  $\mathbb{Y}$ . We define a group for pairs of linked ICD-9 and ICD-10 codes as one in which all ICD-9 codes have the same phcode up to the first decimal point to achieve moderate group sizes. Our final dataset includes



(a) Existing ICD-9-to-10 mapping for rheumatoid arthritis



(b) Estimated ICD-9-to-10 mapping from the isphereMAP method

Figure 5: Plot of the existing GEM (top) and estimated (bottom) mapping from ICD-9 to ICD-10 codes in the group describing rheumatoid arthritis (RA).

12369 linked ICD-9 and ICD-10 SEV pairs belonging to 1494 groups, with 42% one-to-many mapping and 58% one-to-one mapping.

Figure 5 (b) shows the estimated mapping from iSphereMAP, which only differs from the existing GEM mapping in a small amount, and is able to pick up different types of mapping. For comparison, we also used the MT method with and without phecode-group structure in estimation of  $\Pi$ . Using the phecode-group information, the MT method correctly matched 1329 (19%) code-pairs among the 7096 code-pairs correctly identified as one-to-one mapping. Note that the MT method estimates all mappings as one-to-one. However, the match rate is only 0.6% without group information. In contrast, our iSphereMAP correctly matched 2107 (53%) code-pairs among the 3988 (32%) code-pairs correctly identified as one-to-one mapping. In addition, our method can further identify 84% (4412) of the one-to-many mapping cases among 5273 one-to-many mappings in total.

## 6 Discussion

Data-driven semantic embeddings such as ICD code-SEVs are powerful approaches to learning the interpretation of medical codes in routine clinical practice which may differ when endorsed by different providers. We propose a novel code translation method with imperfectly linked embeddings by casting the translation problem into a statistical problem of spherical regression under mismatch. We detail the iSphereMAP algorithm for estimating the translation matrix  $\mathbb{W}$  and the mapping matrix  $\mathbf{\Pi}$  and provide theoretical guarantees. In particular, we detail the extent of mismatch under which one may obtain a consistent estimate of  $\mathbb{W}$ , and demonstrate that removing identified mismatched data based on the sparse estimate of  $\mathbf{\Pi}$  yields an improved estimator for  $\mathbb{W}$ . In addition, we characterized conditions under which the support and magnitude of the mapping matrix  $\mathbf{\Pi}$  can be recovered. Unlike existing methods in the literature on regression with mismatched data and machine translation, the iSphereMAP procedure allows for both one-to-one and one-to-many mapping, and can incorporate group structure when group information is available. Our method performs substantially better than methods limited to one-to-one correspondence and without using grouping information. Our methodological framework is particularly appealing because it can be extended to a wide range of applications, including confounding adjustment via text matching using text data in social science (Roberts et al. 2018, Mozer et al. 2018), and cross-language record linkage (Song et al. 2016, McNamee et al. 2011).

The model selection consistency of  $\mathbf{\Pi}$  currently relies on an approximately noiseless condition where the noise level  $\eta_{\kappa,p} = o(1)$ , for which a sufficient condition is  $\kappa \rightarrow \infty$ ,  $p = o(\kappa)$ , and  $p \geq 4$ . A similar condition that the signal-to-noise ratio goes to infinity was required in Pananjady et al. (2016). The seemingly stringent condition is in fact reasonable because in practice, normalization of the original data to unit length often substantially reduces the noise in the data. Our findings established a theoretical basis for future research on weaker conditions for mapping recovery. When the number of groups  $K$  is relatively small such that some group size  $n_k$  is larger than  $p$ , we may not be able to obtain an initial OLS estimate of  $\mathbf{\Pi}$ . In this case, one may consider the alternative sparsity condition that  $\|\mathbf{\Pi} - \mathbb{I}\|_1$  is small, under which shrinkage estimators such as the LASSO can be used to obtain  $\tilde{\mathbf{\Pi}}$ . Modified iSphereMAP procedure under such settings warrants future research.

## SUPPLEMENTARY MATERIAL

We first provide detailed tail analysis of the vMF distribution in Section A, which is useful for subsequent analysis of error terms. The main theorems are proved in Section B and all supporting lemmas are proved in Section C. Additional simulation results are in Section D.

### A Tail analysis of the vMF distribution

**Proposition A.1.** *Let  $\boldsymbol{\mu} \in \mathbb{S}^{p-1}$ ,  $\mathbf{Z} \sim \text{vMF}_{\boldsymbol{\mu}, \kappa, p}$ , and  $\boldsymbol{\epsilon} = \mathbf{Z} - \boldsymbol{\mu}$ . Then, for  $p \geq 4$  and  $\frac{p-1}{2\kappa} \leq \delta \leq 2$ , the following statements hold.*

1.  $P(\boldsymbol{\epsilon}^\top \boldsymbol{\mu} \leq -\delta) \leq \exp\{-\delta\kappa + \frac{1}{2}(p-1)(\log \kappa + 1) - \frac{1}{2}(p-1)\log(\frac{\frac{1}{2}(p-1)}{\delta})\};$
2.  $P(\|\boldsymbol{\epsilon}\|_2 \geq \sqrt{2\delta}) \leq \exp\{-\delta\kappa + \frac{1}{2}(p-1)(\log \kappa + 1) - \frac{1}{2}(p-1)\log(\frac{\frac{1}{2}(p-1)}{\delta})\}.$
3. *If we have  $Q_1, \dots, Q_m$  be i.i.d copies of  $\|\boldsymbol{\epsilon}\|_2^2$ , then for  $s \geq 0$ ,*

$$P\left\{\sum_{i=1}^m Q_i \geq \frac{m(p-1)}{\kappa} + \frac{m(p-1)}{\kappa}s\right\} \leq \exp\left\{-\frac{m(p-1)}{2}(s - \log(1+s))\right\}. \quad (\text{A.1})$$

4. *Let  $\{Q_{k,l}, k = 1, \dots, K, l = 1, \dots, n_k\}$  be  $n = \sum_{k=1}^K n_k$  i.i.d realizations of  $\|\boldsymbol{\epsilon}\|_2^2$ . Then, for each  $t > 0$ ,*

$$P\left\{\max_{1 \leq k \leq K} \sum_{l=1}^{n_k} Q_{k,l} \geq \frac{n_{\max}(p-1)}{\kappa}(1+s_t)\right\} \leq e^{-t}, \quad (\text{A.2})$$

where  $n_{\max} = \max_{1 \leq k \leq K} n_k$ ,  $s_t \geq 0$  is the unique solution to  $s_t - \log(1+s_t) = \{2(\log K + t)\}/\{(p-1)n_{\min}\}$  and  $n_{\min} = \min_{1 \leq k \leq K} n_k$ . In particular, if  $4 \log K \leq (p-1)n_{\min}$  and  $t = \log K$ , then  $s_t \leq 3$  and

$$P\left(\max_{1 \leq k \leq K} \sum_{l=1}^{n_k} Q_{k,l} \geq \frac{4n_{\max}(p-1)}{\kappa}\right) \leq \frac{1}{K}. \quad (\text{A.3})$$

**Remark A.1.** *The second tail bound implies that  $\|\boldsymbol{\epsilon}\|_2^2 = O_p(p/\kappa)$  and  $\boldsymbol{\epsilon}^\top \boldsymbol{\mu} = O_p(p/\kappa)$ .*

**Remark A.2.** *For  $1 \leq p \leq 3$ , less sharp tail bounds can also be developed.*

*Proof of Proposition A.1.* Without loss of generality, we assume  $\boldsymbol{\mu} = (1, 0, \dots, 0)$ . Then,  $\boldsymbol{\epsilon} = (Z_1 - 1, 0, \dots, 0)$ , and  $P(\boldsymbol{\epsilon}^\top \boldsymbol{\mu} \leq -\delta) = P(1 - Z_1 \geq \delta)$ . Using the Chernoff bound (Chernoff 1952), we can see that for all  $\lambda > 0$ ,

$$P(1 - Z_1 \geq \delta) \leq e^{-\lambda\delta} e^\lambda \mathbb{E}(e^{-\lambda Z_1}) = e^{\lambda(1-\delta)} \mathbb{E}(e^{-\lambda Z_1}). \quad (\text{A.4})$$

We proceed to calculate the moment generating function  $\mathbb{E}(e^{-\lambda Z_1})$ . Let  $f_{Z_1}(z_1)$  be the density function of  $Z_1$ . According to the density function of  $\mathbf{Z}$ , we have the marginal density,

$$f_{Z_1}(z_1) = C_p(\kappa) \exp(\kappa z_1) \omega_{p-2} \left( \sqrt{1 - z_1^2} \right), \quad (\text{A.5})$$

where  $\omega_d(r)$  denotes the surface area of a  $d - 1$ -dimensional sphere (living in a  $d$ -dimensional space) with the radius  $r$ , and  $C_p(\kappa) = \kappa^{p/2-1} / \{(2\pi)^{p/2} B_{p/2-1}(\kappa)\}$  is the normalizing constant for vMF distribution, and  $B_\nu(x)$  denotes the modified Bessel function. Then,

$$\begin{aligned} \mathbb{E}(e^{-\lambda Z_1}) &= \int_{-1}^1 e^{-\lambda z_1} C_p(\kappa) \exp(\kappa z_1) \omega_{p-2}(\sqrt{1 - z_1^2}) dz_1 \\ &= \frac{C_p(\kappa)}{C_p(\kappa - \lambda)} = \left( \frac{\kappa}{\kappa - \lambda} \right)^\nu \frac{B_\nu(\kappa - \lambda)}{B_\nu(\kappa)}, \end{aligned} \quad (\text{A.6})$$

where we let  $\nu = \frac{p}{2} - 1$ . Combining this with (A.4), we have

$$P(1 - Z_1 \geq \delta) \leq e^{-\lambda\delta} e^\lambda \left( \frac{\kappa}{\kappa - \lambda} \right)^\nu \frac{B_\nu(\kappa - \lambda)}{B_\nu(\kappa)}. \quad (\text{A.7})$$

We use the following upper bound of  $\frac{B_\nu(\kappa - \lambda)}{B_\nu(\kappa)}$ , which is the equation (2.6) in Baricz (2010).

For all  $\nu \geq \frac{1}{2}$  and  $0 < x < y$ ,

$$\frac{B_\nu(x)}{B_\nu(y)} < e^{x-y} \left( \frac{y}{x} \right)^{1/2}.$$

Setting  $x = \kappa - \lambda$  and  $y = \kappa$  in the above display and combining it with (A.7), we have

$$P(1 - Z_1 \geq \delta) \leq \inf_{0 \leq \lambda \leq \kappa} e^{-\lambda\delta} \left( \frac{\kappa}{\kappa - \lambda} \right)^{\nu + \frac{1}{2}}.$$



If  $\kappa - \frac{\nu + \frac{1}{2}}{\delta} \geq 0$ ,

$$\inf_{0 \leq \lambda \leq \kappa} e^{-\lambda \delta} \left( \frac{\kappa}{\kappa - \lambda} \right)^{\nu + \frac{1}{2}} = \exp \left\{ -\delta \kappa + (\nu + \frac{1}{2})(\log \kappa + 1) - (\nu + \frac{1}{2}) \log \left( \frac{\nu + \frac{1}{2}}{\delta} \right) \right\},$$

where the minimum is achieved at  $\lambda = \kappa - \frac{\nu + \frac{1}{2}}{\delta}$ . Summarizing the above results, we have

$$P(\boldsymbol{\epsilon}^\top \boldsymbol{\mu} \leq -\delta) \leq \exp \left\{ -\delta \kappa + \frac{1}{2}(p-1)(\log \kappa + 1) - \frac{1}{2}(p-1) \log \left( \frac{\frac{1}{2}(p-1)}{\delta} \right) \right\} \quad (\text{A.8})$$

for  $p \geq 4$  and  $\delta \geq \frac{p-1}{2\kappa}$ . The tail bound of  $\|\boldsymbol{\epsilon}\|_2$  is straightforward based on the above inequality, because  $\|\boldsymbol{\epsilon}\|_2^2 = 2(1 - \boldsymbol{\mu}^\top \mathbf{Z})$ .

To establish (A.1), we note that from a similar Chernoff bound,

$$P\left(\sum_{i=1}^m Q_i \geq 2m\delta\right) \leq \inf_{\lambda \geq 0} \left( e^{-\lambda \delta} \left( \frac{\kappa}{\kappa - \lambda} \right)^{\nu + \frac{1}{2}} \right)^m.$$

for  $\delta \geq \frac{p-1}{2\kappa}$ . According to (A.8), the above display is simplified as

$$P\left(\sum_{i=1}^m Q_i \geq 2m\delta\right) \leq \exp \left\{ m \left( -\delta \kappa + \frac{1}{2}(p-1)(\log \kappa + 1) - \frac{1}{2}(p-1) \log \left( \frac{\frac{1}{2}(p-1)}{\delta} \right) \right) \right\}.$$

Let  $\delta = \frac{p-1}{2\kappa}(1+s)$  in the above display for  $s \geq 0$  and simplifying it, we arrive at

$$P\left(\sum_{i=1}^m Q_i \geq 2m \frac{p-1}{2\kappa}(1+s)\right) \leq \exp \left\{ -\frac{m(p-1)}{2}(s - \log(1+s)) \right\}. \quad (\text{A.9})$$

For (A.2), we first observe that for each  $k$ ,  $1 \leq k \leq K$ , according to (A.1), we have

$$P\left(\sum_{l=1}^{n_k} Q_{k,l} \geq \frac{n_k(p-1)}{\kappa}(1+s_t)\right) \leq \exp \left\{ -\frac{n_k}{n_{\min}}(\log K + t) \right\} \leq e^{-t}/K.$$

This further gives

$$P\left(\sum_{l=1}^{n_k} Q_{k,l} \geq \frac{n_{\max}(p-1)}{\kappa}(1+s_t)\right) \leq K^{-1}e^{-t}. \quad (\text{A.10})$$

By the union bound, we have

$$P \left\{ \max_{1 \leq k \leq K} \sum_{l=1}^{n_k} Q_{k,l} \geq \frac{n_{\max}(p-1)}{\kappa}(1+s_t) \right\} \leq \sum_{i=1}^K P \left\{ \sum_{j=1}^{n_k} Q_{k,l} \geq \frac{n_{\max}(p-1)}{\kappa}(1+s_t) \right\} \leq e^{-t},$$

where the last inequality is obtained by (A.10). This completes the proof for (A.2).

If  $4 \log K \leq (p-1)n_{\min}$  and  $t = \log K$ , then  $s_t - \log(1+s_t) \leq 1$ . It follows that  $s_t < 3$  and

$$P \left\{ \max_{1 \leq k \leq K} \sum_{j=1}^{n_k} Q_{k,l} \geq \frac{4n_{\max}(p-1)}{\kappa} \right\} \leq P \left\{ \max_{1 \leq k \leq K} \sum_{j=1}^{n_k} Q_{k,l} \geq \frac{n_{\max}(p-1)(1+s_t)}{\kappa} \right\} \leq e^{-t} = \frac{1}{K}.$$

□

## B Proof of theorems and corollaries

### B.1 Proof of Theorem 1

*Proof of Theorem 1.* Write  $\boldsymbol{\epsilon}_i = \mathbf{Y}_i - \gamma_{\kappa,p} \mathbb{W}^\top (\boldsymbol{\Pi}_i \mathbb{X})^\top$  and  $\mathbb{V} = \mathbb{Y} - E(\mathbb{Y}) = (\boldsymbol{\epsilon}_1, \dots, \boldsymbol{\epsilon}_n)^\top$ , where

$$\gamma_{\kappa,p} = \frac{B'_{p/2-1}(\kappa)}{2B_{p/2-1}(\kappa)} - \frac{p/2-1}{\kappa}.$$

We have

$$\mathbb{Y} = \gamma_{\kappa,p} \boldsymbol{\Pi} \mathbb{X} \mathbb{W} + \mathbb{V} = \gamma_{\kappa,p} \mathbb{X} \mathbb{W} + \gamma_{\kappa,p} (\boldsymbol{\Pi} - \mathbb{I}) \mathbb{X} \mathbb{W} + \mathbb{V}. \quad (\text{B.1})$$

Recall that we write  $\mathcal{U}(A) = A(A^\top A)^{-1/2}$  for the polar decomposition of  $A$ . Then, by definition,

$$\widehat{\mathbb{W}}^{[1]} = \mathcal{U}(\mathbb{X}^\top \mathbb{Y}) = \mathcal{U}(\gamma_{\kappa,p} \mathbb{X}^\top \mathbb{X} \mathbb{W} + \Delta), \quad \text{where } \Delta = \gamma_{\kappa,p} \mathbb{X}^\top (\boldsymbol{\Pi} - \mathbb{I}) \mathbb{X} \mathbb{W} + \mathbb{X}^\top \mathbb{V}. \quad (\text{B.2})$$

On the other hand, since  $\mathbb{X}^\top \mathbb{X}$  is positive definite with smallest eigenvalue  $\sigma_p(\mathbb{X}) > 0$ ,

$$\mathcal{U}(\gamma_{\kappa,p} \mathbb{X}^\top \mathbb{X} \mathbb{W}) = \mathbb{X}^\top \mathbb{X} \mathbb{W} \mathbb{W}^\top (\mathbb{X}^\top \mathbb{X})^{-1} \mathbb{W} = \mathbb{W}. \quad (\text{B.3})$$

(B.2) and (B.3) together imply

$$\widehat{\mathbb{W}}^{(1)} - \mathbb{W} = \mathcal{U}(\gamma_{\kappa,p} \mathbb{X}^\top \mathbb{X} \mathbb{W} + \Delta) - \mathcal{U}(\gamma_{\kappa,p} \mathbb{X}^\top \mathbb{X} \mathbb{W}). \quad (\text{B.4})$$

We proceed to obtain an upper bound on  $\|\mathcal{U}(\gamma_{\kappa,p} \mathbb{X}^\top \mathbb{X} \mathbb{W} + \Delta) - \mathcal{U}(\gamma_{\kappa,p} \mathbb{X}^\top \mathbb{X} \mathbb{W})\|$ , where  $\|\cdot\|$  denotes a unitary invariant matrix norm. We use results in Lemma B.1, which is a slight modification of Theorem 2.4 in Mathias (1993).

**Lemma B.1** (Modification of Theorem 2.4 in Mathias (1993)). *Let  $A, \Delta$  be two  $p \times p$  real matrices. Assume that  $\sigma_p(A) - \sigma_1(\Delta) > 0$ . Then, for any unitary invariant norm  $\|\cdot\|$ ,*

$$\|\mathcal{U}(A + \Delta) - \mathcal{U}(A)\| \leq 2[\sigma_p(A) + \sigma_{p-1}(A) - 2\sigma_1(\Delta)]^{-1} \|\Delta\|.$$

Let  $A = \gamma_{\kappa,p} \mathbb{X}^\top \mathbb{X} \mathbb{W}$  in Lemma B.1. For any unitary invariant norm  $\|\cdot\|$ , we have

$$\|\mathcal{U}(\gamma_{\kappa,p} \mathbb{X}^\top \mathbb{X} \mathbb{W} + \Delta) - \mathcal{U}(\gamma_{\kappa,p} \mathbb{X}^\top \mathbb{X} \mathbb{W})\| \leq (\sigma_p(A) - \sigma_1(\Delta))^{-1} \|\Delta\|. \quad (\text{B.5})$$

To bound the right-hand side of the above display, we note that

$$\sigma_p(A) \geq \gamma_{\kappa,p} \sigma_p(\mathbb{X})^2 \sigma_p(\mathbb{W}) = \gamma_{\kappa,p} \sigma_p(\mathbb{X})^2, \quad (\text{B.6})$$

$$\text{and } \sigma_1(\Delta) \leq \|\Delta\|_F \leq \gamma_{\kappa,p} \|\mathbb{X}^\top (\mathbf{\Pi} - \mathbb{I}) \mathbb{X} \mathbb{W}\|_F + \|\mathbb{X}^\top \mathbb{V}\|_F \quad (\text{B.7})$$

Recall that  $\mathcal{D} \equiv \mathcal{D}(\mathbf{\Pi}, \mathbb{I}) = \{i \in [n] : \mathbf{\Pi}_i \neq \mathbb{I}_i\}$  indexes the mismatched rows. Then,

$$\begin{aligned} \|\mathbb{X}^\top (\mathbf{\Pi} - \mathbb{I}) \mathbb{X}\|_F &= \|(\mathbb{X}_{[\mathcal{D},:]})^\top (\mathbf{\Pi}_{[\mathcal{D},]} - \mathbb{I}_{[\mathcal{D},]}) \mathbb{X}\|_F \leq \|\mathbb{X}_{[\mathcal{D},]}\|_F \|(\mathbf{\Pi}_{[\mathcal{D},]} - \mathbb{I}_{[\mathcal{D},]}) \mathbb{X}\|_F \\ &\leq \|\mathbb{X}_{[\mathcal{D},]}\|_F \{\|\mathbf{\Pi}_{[\mathcal{D},]} \mathbb{X}\|_F + \|\mathbb{I}_{[\mathcal{D},]} \mathbb{X}\|_F\} = 2n_{\text{mis}}. \end{aligned} \quad (\text{B.8})$$

For the last line of the above display, we used the spherical assumption and obtain that

$\|\mathbb{X}_{[\mathcal{D},]}\|_F = \sqrt{n_{\text{mis}}}$  and  $\|\mathbf{\Pi}_{[\mathcal{D},]} \mathbb{X}\|_F = \sqrt{n_{\text{mis}}}$ . Combining (B.6), (B.5), and (B.8), we have

$$\|\mathcal{U}(\mathbb{X}^\top \mathbb{X} \mathbb{W} + \Delta) - \mathcal{U}(\mathbb{X}^\top \mathbb{X} \mathbb{W})\| \leq \{\gamma_{\kappa,p} \sigma_p(\mathbb{X})^2 - 2\gamma_{\kappa,p} n_{\text{mis}} - \|\mathbb{X}^\top \mathbb{V}\|_F\}^{-1} \|\Delta\|.$$

That is,

$$\|\widehat{\mathbb{W}}^{[1]} - \mathbb{W}\| \leq \{\gamma_{\kappa,p}\sigma_p(\mathbb{X})^2 - 2\gamma_{\kappa,p}n_{\text{mis}} - \|\mathbb{X}^\top \mathbb{V}\|_F\}^{-1} \|\Delta\|.$$

In particular, if we take  $\|\cdot\|$  to be  $\|\cdot\|_F$  in the above inequality, then

$$\|\widehat{\mathbb{W}}^{[1]} - \mathbb{W}\|_F \leq \{\gamma_{\kappa,p}\sigma_p(\mathbb{X})^2 - 2\gamma_{\kappa,p}n_{\text{mis}} - \|\mathbb{X}^\top \mathbb{V}\|_F\}^{-1} (2\gamma_{\kappa,p}n_{\text{mis}} + \|\mathbb{X}^\top \mathbb{V}\|_F). \quad (\text{B.9})$$

To analyze the tail behavior of  $\|\mathbb{X}^\top \mathbb{V}\|_F$ , we note that

$$\mathbb{E}(\|\mathbb{X}^\top \mathbb{V}\|_F^2) = \mathbb{E}(\text{tr}(\mathbb{V}^\top \mathbb{X} \mathbb{X}^\top \mathbb{V})) = \mathbb{E}(\text{tr}(\mathbb{X} \mathbb{X}^\top \mathbb{V} \mathbb{V}^\top)) = \text{tr}(\mathbb{X} \mathbb{X}^\top \mathbb{E}[\mathbb{V} \mathbb{V}^\top]). \quad (\text{B.10})$$

Since  $\mathbb{V} = (\boldsymbol{\epsilon}_1, \dots, \boldsymbol{\epsilon}_n)^\top$  and  $\boldsymbol{\epsilon}_i$ 's are centered and independent random vectors, we have

$$\mathbb{E}[\mathbb{V} \mathbb{V}^\top] = (\mathbb{E} \boldsymbol{\epsilon}_i^\top \boldsymbol{\epsilon}_j)_{1 \leq i, j \leq n} = \text{diag}(\mathbb{E}(\|\boldsymbol{\epsilon}_1\|_2^2), \dots, \mathbb{E}(\|\boldsymbol{\epsilon}_n\|_2^2)). \quad (\text{B.11})$$

From Lemma C.1 in Appendix C, the distribution of  $\|\boldsymbol{\epsilon}_i\|_2^2$  does not depend on  $\boldsymbol{\mu}$  and

$$\mathbb{E}[\mathbb{V} \mathbb{V}^\top] = (\mathbb{E} \boldsymbol{\epsilon}_i^\top \boldsymbol{\epsilon}_j)_{1 \leq i, j \leq n} = (1 - \gamma_{\kappa,p}^2) \mathbb{I}_n. \quad (\text{B.12})$$

On the other hand, the diagonal elements of  $\mathbb{X} \mathbb{X}^\top$  are all ones because of the spherical assumption. Combining this fact with (B.10) and (B.12), we arrive at

$$\mathbb{E}(\|\mathbb{X}^\top \mathbb{V}\|_F^2) = (1 - \gamma_{\kappa,p}^2) \text{tr}(\mathbb{X} \mathbb{X}^\top) = n(1 - \gamma_{\kappa,p}^2). \quad (\text{B.13})$$

Now we apply Chebyshev inequality to  $\|\mathbb{X}^\top \mathbb{V}\|_F$  and obtain that for all  $t > 0$

$$P(\|\mathbb{X}^\top \mathbb{V}\|_F \geq t) \leq t^{-2} n(1 - \gamma_{\kappa,p}^2), \quad (\text{B.14})$$

or, equivalently,

$$P(\|\mathbb{X}^\top \mathbb{V}\|_F \geq t \sqrt{n(1 - \gamma_{\kappa,p}^2)}) \leq t^{-2} \quad (\text{B.15})$$

for all  $t > 0$ . Combining (B.14) and (B.9), we arrive at

$$\|\widehat{\mathbb{W}}^{[1]} - \mathbb{W}\|_F \leq \frac{2\gamma_{\kappa,p}n_{\text{mis}} + t\sqrt{n(1 - \gamma_{\kappa,p}^2)}}{\gamma_{\kappa,p}\sigma_p(\mathbb{X})^2 - 2\gamma_{\kappa,p}n_{\text{mis}} - t\sqrt{n(1 - \gamma_{\kappa,p}^2)}} \quad (\text{B.16})$$

with probability that is at least  $1 - 1/t^2$ .

□

## B.2 Proof of Corollary 1

*Proof of Corollary 1.* The proof for the case where both  $p$  and  $\kappa$  are fixed is straightforward because  $\rho < \gamma_{\kappa,p} < 1$  is a constant. Now we consider the case when  $\kappa \rightarrow \infty$  and  $p \geq 4$ . By the assumption that  $\gamma_{\kappa,p} > \rho$  is bounded away from zero, we have

$$\|\widehat{\mathbb{W}}^{[1]} - \mathbb{W}\|_F \leq \frac{2n_{\text{mis}} + t\sqrt{n\eta_{\kappa,p}/\gamma_{\kappa,p}}}{\sigma_p(\mathbb{X})^2 - 2n_{\text{mis}} - t\sqrt{n\eta_{\kappa,p}/\gamma_{\kappa,p}}}$$

with probability at least  $1 - 1/t^2$ . Therefore, we have

$$\|\widehat{\mathbb{W}}^{[1]} - \mathbb{W}\|_F = O_P\left(\frac{\sqrt{n\eta_{\kappa,p}} + n_{\text{mis}}}{\sigma_p(\mathbb{X})^2}\right)$$

if  $\sqrt{n\eta_{\kappa,p}} = o(\sigma_p(\mathbb{X})^2)$  and  $n_{\text{mis}} = o(\sigma_p(\mathbb{X})^2)$ . In particular, when  $n_{\text{mis}} = o(\sigma_p(\mathbb{X}))$  and  $\sqrt{np/\kappa} = o(\sigma_p(\mathbb{X}))$ , we have  $\|\widehat{\mathbb{W}}^{[1]} - \mathbb{W}\|_F = o_p(1)$ .

□

## B.3 Proof of Theorem 2

*Proof of Theorem 2.* For any  $k \in \{1, \dots, K\}$ , let  $\mathbb{U}_{[G_k, :]} = \mathbb{Y}_{[G_k, :]} - \mathbf{\Pi}_{[G_k, G_k]}\mathbb{X}_{[G_k, :]} \mathbb{W}$  be the  $n_k \times p$  residual matrix. The OLS estimator for  $\mathbf{\Pi}^k$  is

$$\tilde{\mathbf{\Pi}}^k \equiv \tilde{\mathbf{\Pi}}_{[G_k, G_k]}^\top = (\mathbb{X}_{[G_k, :]} \mathbb{X}_{[G_k, :]}^\top)^{-1} \mathbb{X}_{[G_k, :]} \widehat{\mathbb{W}}^{[1]} \mathbb{Y}_{[G_k, :]}^\top = \mathbb{Y}_{[G_k, :]} (\widehat{\mathbb{W}}^{[1]})^\top \mathbb{X}_{[G_k, :]}^\top (\mathbb{X}_{[G_k, :]} \mathbb{X}_{[G_k, :]}^\top)^{-1}.$$

Let  $\Delta \mathbb{W} = \widehat{\mathbb{W}}^{[1]} - \mathbb{W}$ , then

$$\begin{aligned}\widetilde{\boldsymbol{\Pi}}^k &= (\boldsymbol{\Pi}^k \mathbb{X}_{[G_k, :]} \mathbb{W} + \mathbb{U}_{[G_k, :]}) (\mathbb{W}^\top + \Delta \mathbb{W}^\top) \mathbb{X}_{[G_k, :]}^\top (\mathbb{X}_{[G_k, :]} \mathbb{X}_{[G_k, :]}^\top)^{-1} \\ &= \boldsymbol{\Pi}^k + \boldsymbol{\Pi}^k \mathbb{X}_{[G_k, :]} \mathbb{W} (\Delta \mathbb{W})^\top \mathbb{X}_{[G_k, :]}^\top (\mathbb{X}_{[G_k, :]} \mathbb{X}_{[G_k, :]}^\top)^{-1} \\ &\quad + \mathbb{U}_{[G_k, :]} \mathbb{W}^\top \mathbb{X}_{[G_k, :]}^\top (\mathbb{X}_{[G_k, :]} \mathbb{X}_{[G_k, :]}^\top)^{-1} + \mathbb{U}_{[G_k, :]} (\Delta \mathbb{W})^\top \mathbb{X}_{[G_k, :]}^\top (\mathbb{X}_{[G_k, :]} \mathbb{X}_{[G_k, :]}^\top)^{-1}.\end{aligned}$$

In what follows, we find an upper bound of

$$\begin{aligned}& \|\boldsymbol{\Pi}^k \mathbb{X}_{[G_k, :]} \mathbb{W} (\Delta \mathbb{W})^\top \mathbb{X}_{[G_k, :]}^\top (\mathbb{X}_{[G_k, :]} \mathbb{X}_{[G_k, :]}^\top)^{-1}\|_F \\ &+ \|\mathbb{U}_{[G_k, :]} \mathbb{W}^\top \mathbb{X}_{[G_k, :]}^\top (\mathbb{X}_{[G_k, :]} \mathbb{X}_{[G_k, :]}^\top)^{-1}\|_F + \|\mathbb{U}_{[G_k, :]} (\Delta \mathbb{W})^\top \mathbb{X}_{[G_k, :]}^\top (\mathbb{X}_{[G_k, :]} \mathbb{X}_{[G_k, :]}^\top)^{-1}\|_F.\end{aligned}$$

Fro the first term, we note that  $\sigma_1\{\mathbb{X}_{[G_k, :]}^\top (\mathbb{X}_{[G_k, :]} \mathbb{X}_{[G_k, :]}^\top)^{-1}\} = \sigma_1\{(\mathbb{X}_{[G_k, :]}^\top \mathbb{X}_{[G_k, :]}^\top)^{-1}\}^{1/2} = \sigma_{n_k}(\mathbb{X}_{[G_k, :]})^{-1}$  and hence

$$\begin{aligned}\|\boldsymbol{\Pi}^k \mathbb{X}_{[G_k, :]} \mathbb{W} (\Delta \mathbb{W})^\top \mathbb{X}_{[G_k, :]}^\top (\mathbb{X}_{[G_k, :]} \mathbb{X}_{[G_k, :]}^\top)^{-1}\|_F &\leq \|\boldsymbol{\Pi}^k \mathbb{X}_{[G_k, :]}\|_2 \|\Delta \mathbb{W}\|_F \|\mathbb{X}_{[G_k, :]} (\mathbb{X}_{[G_k, :]} \mathbb{X}_{[G_k, :]}^\top)^{-1}\|_2 \\ &\leq \sigma_{n_k}(\mathbb{X}_{[G_k, :]})^{-1} \sigma_1(\boldsymbol{\Pi}^k \mathbb{X}_{[G_k, :]}) \|\Delta \mathbb{W}\|_F,\end{aligned}$$

where for a matrix  $\mathbf{A}$ ,  $\|\mathbf{A}\|_2$  denotes its spectral norm. For the second term, we have

$$\|\mathbb{U}_{[G_k, :]} \mathbb{W}^\top \mathbb{X}_{[G_k, :]}^\top (\mathbb{X}_{[G_k, :]} \mathbb{X}_{[G_k, :]}^\top)^{-1}\|_F \leq \sigma_{n_k}(\mathbb{X}_{[G_k, :]})^{-1} \|\mathbb{U}_{[G_k, :]}\|_F.$$

For the third term, we have

$$\|\mathbb{U}_{[G_k, :]} (\Delta \mathbb{W})^\top \mathbb{X}_{[G_k, :]}^\top (\mathbb{X}_{[G_k, :]} \mathbb{X}_{[G_k, :]}^\top)^{-1}\|_F \leq \sigma_{n_k}(\mathbb{X}_{[G_k, :]})^{-1} \|\mathbb{U}_{[G_k, :]}\|_F \|\Delta \mathbb{W}\|_F.$$

Combining these inequality, we have

$$\|\widetilde{\boldsymbol{\Pi}}^k - \boldsymbol{\Pi}_{[G_k, G_k]}\|_F \leq \sigma_{n_k}(\mathbb{X}_{[G_k, :]})^{-1} \{\|\mathbb{U}_{[G_k, :]}\|_F (1 + \|\Delta \mathbb{W}\|_F) + \sigma_1(\boldsymbol{\Pi}^k \mathbb{X}_{[G_k, :]}) \|\Delta \mathbb{W}\|_F\}.$$

We combine our analysis for different and arrive at

$$\begin{aligned}
& \max_{1 \leq k \leq K} \|\tilde{\mathbf{\Pi}}^k - \mathbf{\Pi}^k\|_F \\
& \leq \left[ \min_{1 \leq k \leq K} \sigma_{n_k}(\mathbb{X}_{[G_k, :]}) \right]^{-1} \left\{ \max_{1 \leq k \leq K} \|\mathbb{U}_{[G_k, :]}\|_F (1 + \|\Delta \mathbb{W}\|_F) + \max_{1 \leq k \leq K} \sigma_1(\mathbf{\Pi}^k \mathbb{X}_{[G_k, :]}) \|\Delta \mathbb{W}\|_F \right\} \\
& = \left[ \min_{1 \leq k \leq K} \sigma_{n_k}(\mathbb{X}_{[G_k, :]}) \right]^{-1} \left\{ (1 + \|\Delta \mathbb{W}\|_F) \max_{1 \leq k \leq K} \|\mathbb{U}_{[G_k, :]}\|_F + \|\Delta \mathbb{W}\|_F \max_{1 \leq k \leq K} \sqrt{n_k} \right\}.
\end{aligned}$$

We proceed to analyzing the probabilistic properties of the above display. From Corollary 1, we know that under the assumptions of Corollary 1,

$$\|\Delta \mathbb{W}\|_F = O_p(\sigma_p(\mathbb{X})^{-2}(\sqrt{n\eta_{\kappa,p}} + n_{\text{mis}})) = o_p(1).$$

For  $\max_{1 \leq k \leq K} \|\mathbb{U}_{[G_k, :]}\|_F$ , we apply (A.2) in Proposition A.1. Then, we have that with probability at least  $1 - \frac{1}{K}$ ,

$$\max_{1 \leq k \leq K} \|\mathbb{U}_{[G_k, :]}\|_F \leq 2 \max_{1 \leq k \leq K} \sqrt{n_k} \left( \frac{p-1}{\kappa} \right)^{1/2},$$

given that  $4 \log K \leq (p-1)n_{\min}$ . Combining these, we have with the probability going to one,

$$\max_{1 \leq k \leq K} \|\tilde{\mathbf{\Pi}}^k - \mathbf{\Pi}^k\|_F \leq 4c_n, \text{ where } c_n = \frac{\max_{1 \leq k \leq K} \sqrt{n_k} \left\{ \left( \frac{p}{\kappa} \right)^{1/2} + \sigma_p(\mathbb{X})^{-2} (\sqrt{n\eta_{\kappa,p}} + n_{\text{mis}}) \right\}}{\min_{1 \leq k \leq K} \sigma_{n_k}(\mathbb{X}_{[G_k, :]})}.$$

Assuming that  $p = o(\kappa)$ , we further have that with the probability converging to one,

$$\max_{1 \leq k \leq K} \|\tilde{\mathbf{\Pi}}^k - \mathbf{\Pi}^k\|_F \leq 4c_n.$$

which implies that  $\|\tilde{\mathbf{\Pi}} - \mathbf{\Pi}\|_2 = O_p(c_n)$ .

□

## B.4 Proof of Theorem 3

*Proof of Theorem 3.* From Theorems 1 and 2, we have for any  $a_n \rightarrow \infty$ ,  $P(F_n) \rightarrow 1$ , where

$$F_n = \left\{ \max_{1 \leq k \leq K} \|\tilde{\mathbf{\Pi}}_k - \mathbf{\Pi}_k\|_F \leq a_n c_n \text{ and } \|\Delta \mathbb{W}\|_F \leq a_n \sigma_p(\mathbb{X})^{-2} (\sqrt{n \eta_{\kappa, p}} + n_{\text{mis}}) \right\}, \quad (\text{B.17})$$

and  $c_n$  is defined above. From now on, we restrict our analysis on the event  $F_n$  with some suitable choice of  $a_n$ . We first observe that when  $F_n$  occurs, for each row

$$\|\tilde{\mathbf{\Pi}}_{i\cdot} - \mathbf{\Pi}_{i\cdot}\|_2 \leq d_n, \quad (\text{B.18})$$

where  $d_n = a_n c_n$ . We first use Lemma C.2 to show that, if  $\mathbf{\Pi}_{i\cdot} = \mathbb{I}_{j\cdot}$  for some  $j$ , then  $\hat{\mathbf{\Pi}}_{i\cdot}^{[2]} = \mathbb{I}_{j\cdot}$ . In other words, we show that for all  $i \notin \mathcal{C}$ ,  $\hat{\mathbf{\Pi}}_{i\cdot}^{[2]} = \mathbf{\Pi}_{i\cdot} = \mathbb{I}_{j\cdot}$ . Lemma C.2 and (B.18) imply that if  $2d_n < \lambda_n < \frac{1}{2}$  and  $\mathbf{\Pi}_{i\cdot} = \mathbb{I}_{j\cdot}$  for some  $j$ , then we get  $\hat{\mathbf{\Pi}}_{i\cdot}^{[2]} = \mathbb{I}_{j\cdot}$ . This result holds for all rows  $i \notin \mathcal{C}$ . Thus, given  $c_n \ll \lambda_n < \frac{1}{2}$ , we have the exact recovery for rows  $i \notin \mathcal{C}$  on the event  $F_n$  with any sequence  $a_n$  such that  $a_n \rightarrow \infty$  and  $a_n \ll \lambda_n / c_n$ .

It remains to show that the hard thresholding does not have any effect on the rows with  $i \in \mathcal{C}$ . We note that

$$\left\| \frac{\tilde{\mathbf{\Pi}}_{i\cdot}}{\|\mathbf{\Pi}_{i\cdot}\|_2} - \frac{\mathbf{\Pi}_{i\cdot}}{\|\mathbf{\Pi}_{i\cdot}\|_2} \right\|_2 \leq \frac{d_n}{\|\mathbf{\Pi}_{i\cdot}\|_2}.$$

Similar to Lemma C.2, we have

$$\cos \left( \frac{\tilde{\mathbf{\Pi}}_{i\cdot}}{\|\mathbf{\Pi}_{i\cdot}\|_2}, \frac{\mathbf{\Pi}_{i\cdot}}{\|\mathbf{\Pi}_{i\cdot}\|_2} \right) \geq 1 - \frac{2d_n}{\|\mathbf{\Pi}_{i\cdot}\|_2}. \quad (\text{B.19})$$

To bound  $\cos(\tilde{\mathbf{\Pi}}_{i\cdot}, \mathbb{I}_{j\cdot})$ , we use Lemma C.3 in Appendix C by setting  $\mathbf{X} = \tilde{\mathbf{\Pi}}_{i\cdot}$ ,  $\mathbf{Y} = \mathbf{\Pi}_{i\cdot}$  and  $\mathbf{Z} = \mathbb{I}_{j\cdot}$ . It follows that

$$\cos(\tilde{\mathbf{\Pi}}_{i\cdot}, \mathbb{I}_{j\cdot}) \leq 1 - \min_{i \in \mathcal{C}} \beta_j + 2\sqrt{\frac{d_n}{\|\mathbf{\Pi}_{i\cdot}\|_2}} = 1 - \mathcal{B}_{\min} + 2\sqrt{\frac{d_n}{\|\mathbf{\Pi}_{i\cdot}\|_2}}.$$



From Lemma C.4,  $\|\mathbf{\Pi}_{i\cdot}\|_2 \geq 1/\sqrt{n_k}$ . Thus, we arrive at

$$\cos(\tilde{\mathbf{\Pi}}_{i\cdot}, \mathbb{I}_{j\cdot}) \leq 1 - \mathcal{B}_{\min} + 2\sqrt{d_n \max_{1 \leq k \leq K} \sqrt{n_k}},$$

which implies

$$1 - \tilde{\beta}_i = \max_{j: j \sim i} \cos(\tilde{\mathbf{\Pi}}_{i\cdot}, \mathbb{I}_{j\cdot}) \leq 1 - \mathcal{B}_{\min} + 2\sqrt{d_n \max_{1 \leq k \leq K} \sqrt{n_k}}.$$

That is,  $\tilde{\beta}_i \geq \mathcal{B}_{\min} - 2\sqrt{d_n \max_{1 \leq k \leq K} \sqrt{n_k}}$ . Because we do hard-thresholding only when  $\tilde{\beta}_i \leq \lambda_n$ , and from the theorem assumptions we have  $\mathcal{B}_{\min} - 2\sqrt{d_n \max_{1 \leq k \leq K} \sqrt{n_k}} > \lambda_n$  for large  $n$ , we can see that the hard-thresholding will not have any effect to the  $i$ 'th row of  $\tilde{\mathbf{\Pi}}$  for sufficiently large  $n$ . This completes our proof for the model selection consistency part.

We proceed to the estimation error bound of  $\hat{\mathbf{\Pi}}_{i\cdot}^{[2]}$  for  $i \in \mathcal{C}$ . Without loss of generality, suppose  $i \in G_k$ . Recall that  $\hat{\mathbf{\Pi}}_{i\cdot}^{[2]} = \xi_i \tilde{\mathbf{\Pi}}_{i\cdot}$ , where  $\xi_i = \|\tilde{\mathbf{\Pi}}_{i\cdot} \mathbb{X} \widehat{\mathbb{W}}^{[1]}\|_2^{-1}$ . Clearly,

$$\|\hat{\mathbf{\Pi}}_{i\cdot}^{[2]} - \mathbf{\Pi}_{i\cdot}\|_2 \leq \|\tilde{\mathbf{\Pi}}_{i\cdot}\|_2 |\xi_i - 1| + \|\tilde{\mathbf{\Pi}}_{i\cdot} - \mathbf{\Pi}_{i\cdot}\|_2 \leq (\|\mathbf{\Pi}_{i\cdot}\|_2 + d_n) |\xi_i - 1| + d_n. \quad (\text{B.20})$$

Now we consider an upper bound on  $|\xi_i - 1|$ . We observe that for  $i \in G_k$ ,

$$\begin{aligned} |1 - 1/\xi_i| &= \left| \|\tilde{\mathbf{\Pi}}_{i\cdot} \mathbb{X} \widehat{\mathbb{W}}^{[1]}\|_2 - 1 \right| \leq \|\tilde{\mathbf{\Pi}}_{i\cdot} \mathbb{X} \widehat{\mathbb{W}}^{[1]} - \mathbf{\Pi}_{i\cdot} \mathbb{X} \mathbb{W}\|_2 \\ &\leq \|\tilde{\mathbf{\Pi}}_{i\cdot} \mathbb{X} \widehat{\mathbb{W}}^{[1]} - \mathbf{\Pi}_{i\cdot} \mathbb{X} \widehat{\mathbb{W}}^{[1]}\|_2 + \|\mathbf{\Pi}_{i\cdot} \mathbb{X} \widehat{\mathbb{W}}^{[1]} - \mathbf{\Pi}_{i\cdot} \mathbb{X} \mathbb{W}\|_2 \\ &\leq d_n \sigma_1(\mathbb{X}_{[G_k, :]}) + \sigma_1(\mathbf{\Pi}_{i\cdot} \mathbb{X}) \|\Delta \mathbb{W}\|_F \leq d_n \sqrt{n_k} + \|\Delta \mathbb{W}\|_F \\ &\leq d_n \sqrt{n_k} + a_n \sigma_p(\mathbb{X})^{-2} (\sqrt{n \eta_{\kappa, p}} + n_{\text{mis}}) \leq 2d_n \sqrt{n_k}. \end{aligned} \quad (\text{B.21})$$

It follows that  $|\xi_i - 1| \leq |1 - 1/\xi_i| / (1/\xi_i) \leq 2d_n \sqrt{n_k} / (1 - 2d_n \sqrt{n_k})$ . Under assumption of the theorem, for  $n$  sufficiently large,  $d_n \sqrt{n_k} < 1/4$ , we have  $|\xi_i - 1| \leq 4d_n \sqrt{n_k} < 1$ . Combining this inequality with (B.20) and the fact that  $d_n \sqrt{n_k} < \frac{1}{4}$  again, we have

$$\|\hat{\mathbf{\Pi}}_{i\cdot}^{[2]} - \mathbf{\Pi}_{i\cdot}\|_2 \leq d_n \{(\|\mathbf{\Pi}_{i\cdot}\|_2 + d_n) 4\sqrt{n_k} + 1\} \leq d_n (4\|\mathbf{\Pi}_{i\cdot}\|_2 \sqrt{n_k} + 2) \leq 6d_n \|\mathbf{\Pi}_{i\cdot}\|_2 \sqrt{n_k}. \quad (\text{B.22})$$

To get the last inequality in the above display, we used Lemma C.4. In particular, if

$c_n \max_{1 \leq k \leq K} \max_{i \in \mathcal{C}, i \in G_k} \|\mathbf{\Pi}_i\|_2 \sqrt{n_k} \rightarrow 0$ , then with  $a_n$  chosen such that  $a_n \rightarrow \infty$  and  $a_n c_n \max_{1 \leq k \leq K} \max_{i \in \mathcal{C}, i \in G_k} \|\mathbf{\Pi}_i\|_2 \sqrt{n_k} \rightarrow 0$ , we have  $d_n \max_{1 \leq k \leq K} \max_{i \in \mathcal{C}, i \in G_k} \|\mathbf{\Pi}_i\|_2 \sqrt{n_k} \rightarrow 0$ , where  $d_n = a_n c_n$ . This together with (B.22) implies that

$$\max_{i \in \mathcal{C}} \|\widehat{\mathbf{\Pi}}_{i \cdot}^{[2]} - \mathbf{\Pi}_{i \cdot}\|_2 \rightarrow 0$$

on the event  $F_n$ . That is, all rows of  $\widehat{\mathbf{\Pi}}_{i \cdot}^{[2]}$  are consistent when  $i \in \mathcal{C}$ .

□

## B.5 Proof of Corollary 2

*Proof of Corollary 2.* The subsample we use to obtain  $\widehat{\mathbb{W}}^{[2]}$  includes  $\mathbb{X}_{[\mathcal{S}(\widehat{\mathbf{\Pi}}^{[2]})] \cdot}$  and

$$\mathbb{Y}_{[\mathcal{S}(\widehat{\mathbf{\Pi}}^{[2]})] \cdot} = \gamma_{\kappa, p} \mathbb{X}_{[\mathcal{S}(\widehat{\mathbf{\Pi}}^{[2]})] \cdot} \mathbb{W} + \gamma_{\kappa, p} (\mathbf{\Pi}_{[\mathcal{S}(\widehat{\mathbf{\Pi}}^{[2]})] \cdot} - \mathbb{I}_{[\mathcal{S}(\widehat{\mathbf{\Pi}}^{[2]})] \cdot}) \mathbb{X} \mathbb{W} + \mathbb{V}_{[\mathcal{S}(\widehat{\mathbf{\Pi}}^{[2]})] \cdot},$$

with sample size  $|\mathcal{S}(\widehat{\mathbf{\Pi}}^{[2]})|$ . Therefore, we have that the refined estimate

$$\begin{aligned} \widehat{\mathbb{W}}^{[2]} &= \mathcal{U}(\mathbb{X}_{[\mathcal{S}(\widehat{\mathbf{\Pi}}^{[2]})] \cdot}^\top \mathbb{Y}_{[\mathcal{S}(\widehat{\mathbf{\Pi}}^{[2]})] \cdot}) \\ &= \mathcal{U}(\gamma_{\kappa, p} \mathbb{X}_{[\mathcal{S}(\widehat{\mathbf{\Pi}}^{[2]})] \cdot}^\top \mathbb{X}_{[\mathcal{S}(\widehat{\mathbf{\Pi}}^{[2]})] \cdot} \mathbb{W} + \gamma_{\kappa, p} \mathbb{X}_{[\mathcal{S}(\widehat{\mathbf{\Pi}}^{[2]})] \cdot}^\top (\mathbf{\Pi}_{[\mathcal{S}(\widehat{\mathbf{\Pi}}^{[2]})] \cdot} - \mathbb{I}_{[\mathcal{S}(\widehat{\mathbf{\Pi}}^{[2]})] \cdot}) \mathbb{X} \mathbb{W} + \mathbb{X}_{[\mathcal{S}(\widehat{\mathbf{\Pi}}^{[2]})] \cdot}^\top \mathbb{V}_{[\mathcal{S}(\widehat{\mathbf{\Pi}}^{[2]})] \cdot}) \end{aligned}$$

Let  $A = \gamma_{\kappa, p} \mathbb{X}_{[\mathcal{S}(\widehat{\mathbf{\Pi}}^{[2]})] \cdot}^\top \mathbb{X}_{[\mathcal{S}(\widehat{\mathbf{\Pi}}^{[2]})] \cdot} \mathbb{W}$ , and

$$\Delta = \gamma_{\kappa, p} \mathbb{X}_{[\mathcal{S}(\widehat{\mathbf{\Pi}}^{[2]})] \cdot}^\top (\mathbf{\Pi}_{[\mathcal{S}(\widehat{\mathbf{\Pi}}^{[2]})] \cdot} - \mathbb{I}_{[\mathcal{S}(\widehat{\mathbf{\Pi}}^{[2]})] \cdot}) \mathbb{X} \mathbb{W} + \mathbb{X}_{[\mathcal{S}(\widehat{\mathbf{\Pi}}^{[2]})] \cdot}^\top \mathbb{V}_{[\mathcal{S}(\widehat{\mathbf{\Pi}}^{[2]})] \cdot}.$$

Then by the same arguments as the proof of Theorem 1, we have  $\mathcal{U}(A) = \mathbb{W}$ , and  $\sigma_p(A) \geq \gamma_{\kappa, p} \sigma_p(\mathbb{X}_{[\mathcal{S}(\widehat{\mathbf{\Pi}}^{[2]})] \cdot})^2$ . In addition, by Lemma 3 we have

$$\|\mathcal{U}(A + \Delta) - \mathcal{U}(A)\|_F \leq (\sigma_p(A) - \sigma_1(\Delta))^{-1} \|\Delta\|_F \leq (\sigma_p(A) - \|\Delta\|_F)^{-1} \|\Delta\|_F.$$

For  $\|\Delta\|_F$ , by the same argument as the proof of Theorem 1, we have

$$\begin{aligned}\|\Delta\|_F &\leq \gamma_{\kappa,p} \|\mathbb{X}_{[\mathcal{S}(\hat{\mathbf{\Pi}}^{[2]})],:}^\top (\mathbf{\Pi}_{[\mathcal{S}(\hat{\mathbf{\Pi}}^{[2]})],:} - \mathbb{I}_{[\mathcal{S}(\hat{\mathbf{\Pi}}^{[2]})],:}) \mathbb{X} \mathbb{W}\|_F + \|\mathbb{X}_{[\mathcal{S}(\hat{\mathbf{\Pi}}^{[2]})],:}^\top \mathbb{V}_{[\mathcal{S}(\hat{\mathbf{\Pi}}^{[2]})],:}\|_F \\ &\leq 2\gamma_{\kappa,p} |\mathcal{D}(\mathbf{\Pi}_{[\mathcal{S}(\hat{\mathbf{\Pi}}^{[2]})],:}, \mathbb{I}_{[\mathcal{S}(\hat{\mathbf{\Pi}}^{[2]})],:})| + \|\mathbb{X}_{[\mathcal{S}(\hat{\mathbf{\Pi}}^{[2]})],:}^\top \mathbb{V}_{[\mathcal{S}(\hat{\mathbf{\Pi}}^{[2]})],:}\|_F\end{aligned}\quad (\text{B.23})$$

Next, define the event  $\mathcal{I} = \{\mathcal{D}(\mathbf{\Pi}_{[\mathcal{S}(\hat{\mathbf{\Pi}}^{[2]})],:}, \mathbb{I}_{[\mathcal{S}(\hat{\mathbf{\Pi}}^{[2]})],:}) = \emptyset\}$ , then for a positive  $t$ , we have  $P(\|\Delta\|_F > t) \leq P(\mathcal{I}^c) + P(\|\Delta\|_F > t, \mathcal{I})$ . First, under the assumptions in Theorem 3,  $P(\mathcal{I}^c) \rightarrow 0$ . Second, by (B.23) we have

$$\begin{aligned}P(\|\Delta\|_F > t, \mathcal{I}) &\leq P(2\gamma_{\kappa,p} |\mathcal{D}(\mathbf{\Pi}_{[\mathcal{S}(\hat{\mathbf{\Pi}}^{[2]})],:}, \mathbb{I}_{[\mathcal{S}(\hat{\mathbf{\Pi}}^{[2]})],:})| + \|\mathbb{X}_{[\mathcal{S}(\hat{\mathbf{\Pi}}^{[2]})],:}^\top \mathbb{V}_{[\mathcal{S}(\hat{\mathbf{\Pi}}^{[2]})],:}\|_F > t, \mathcal{I}) \\ &= P(\|\mathbb{X}_{[\mathcal{S}(\hat{\mathbf{\Pi}}^{[2]})],:}^\top \mathbb{V}_{[\mathcal{S}(\hat{\mathbf{\Pi}}^{[2]})],:}\|_F > t, \mathcal{I}) = P(\|\mathbb{X}_{[\mathcal{S}(\mathbf{\Pi})],:}^\top \mathbb{V}_{[\mathcal{S}(\mathbf{\Pi})],:}\|_F > t, \mathcal{I}) \\ &\leq P(\|\mathbb{X}_{[\mathcal{S}(\mathbf{\Pi})],:}^\top \mathbb{V}_{[\mathcal{S}(\mathbf{\Pi})],:}\|_F > t).\end{aligned}$$

By the Chebyshev inequality, we have

$$P(\|\Delta\|_F > t, \mathcal{I}) \leq \frac{1}{t^2} \mathbb{E}[\|\mathbb{X}_{[\mathcal{S}(\mathbf{\Pi})],:}^\top \mathbb{V}_{[\mathcal{S}(\mathbf{\Pi})],:}\|_F^2] = \frac{1}{t^2} (n - n_{\text{mis}}) \eta_{\kappa,p},$$

where the last equation follows the same argument as (B.13), except the sample size here is  $|\mathcal{S}(\mathbf{\Pi})| = n - n_{\text{mis}}$  rather than  $n$ , with  $\eta_{\kappa,p} = 1 - \gamma_{\kappa,p}^2$ . It follows that

$$P(\|\Delta\|_F > t, \mathcal{I}) \leq \frac{1}{t^2} (n - n_{\text{mis}}) \eta_{\kappa,p} \quad (\text{B.24})$$

Therefore,

$$P\left(\|\widehat{\mathbb{W}}^{[2]} - \mathbb{W}\|_F \geq \frac{t\sqrt{(n - n_{\text{mis}})\eta_{\kappa,p}}}{\gamma_{\kappa,p}\sigma_p(\mathbb{X}_{[\mathcal{S}(\mathbf{\Pi})],:})^2 - t\sqrt{(n - n_{\text{mis}})\eta_{\kappa,p}}}\right) \leq P(\mathcal{I}^c) + 1/t^2, \quad (\text{B.25})$$

which further implies that as  $n$  grows,

$$\|\widehat{\mathbb{W}}^{[2]} - \mathbb{W}\|_F = O_p\left\{\frac{\sqrt{(n - n_{\text{mis}})\eta_{\kappa,p}}}{\gamma_{\kappa,p}\sigma_p(\mathbb{X}_{[\mathcal{S}(\mathbf{\Pi})],:})^2}\right\}.$$

Note that (B.24) holds when assumptions of Theorem 3 are satisfied, under which we have

$$\gamma_{\kappa,p} = 1 + o(1) \text{ and } \eta_{\kappa,p} = O(p/\kappa) = o(1). \quad (\text{B.26})$$

Moreover, by Weyl's perturbation theorem (see, e.g. Stewart & Sun (1990)) and the fact that  $\|\mathbf{X}_i\| = 1, \forall i$ , we have  $\sigma_p(\mathbb{X})^2 - n_{\text{mis}} \leq \sigma_p(\mathbb{X}_{[S(\mathbf{\Pi}),:]})^2 \leq \sigma_p(\mathbb{X})^2$ . By the assumption of Theorem 2 that  $n_{\text{mis}} = o(\sigma_p(\mathbb{X})^2)$ , we know that

$$\sigma_p(\mathbb{X}_{[S(\mathbf{\Pi}),:]})^2 = (1 + o(1))\sigma_p(\mathbb{X})^2. \quad (\text{B.27})$$

Because  $\sqrt{(n - n_{\text{mis}})\eta_{\kappa,p}} < \sqrt{n\eta_{\kappa,p}} = o(\sigma_p(\mathbb{X})^2)$  due to assumptions in Theorem 2, by (B.27) we have

$$\sqrt{(n - n_{\text{mis}})\eta_{\kappa,p}} = o(\sigma_p(\mathbb{X}_{[S(\mathbf{\Pi}),:]})^2). \quad (\text{B.28})$$

Combining (B.25), (B.26), (B.27), and (B.28), we obtain that the error rate is

$$\|\widehat{\mathbb{W}}^{[2]} - \mathbb{W}\|_F = O_p \left\{ \frac{\sqrt{(n - n_{\text{mis}})\eta_{\kappa,p}}}{\sigma_p(\mathbb{X})^2} \right\}. \quad (\text{B.29})$$

□

## C Proof of supporting lemmas

**Lemma 1.** For  $p \geq 4$  and  $\kappa > 0$ ,  $\max\{0, 1 - \frac{p-1}{2\kappa}\} < \gamma_{\kappa,p} < 1$ .

*Proof.* Without loss of generality, assume  $\boldsymbol{\mu} = (1, 0, \dots, 0)$ . Then,  $\gamma_{\kappa,p} = \mathbb{E}(Z_1)$ , where  $\mathbf{Z} = (Z_1, \dots, Z_p)^\top \sim \text{vMF}_{\boldsymbol{\mu}, \kappa, p}$ . The moment generating function of  $Z_1$  as  $M_{Z_1}(\lambda) = C_p(\kappa)/C_p(\kappa + \lambda)$  as shown in the proof of Proposition A.1. Thus, we have

$$\gamma_{\kappa,p} = \mathbb{E}(Z_1) = (\log M_{Z_1}(\lambda))'|_{\lambda=0} = -\frac{C'_p(\kappa)}{C_p(\kappa)} = \frac{B'_{p/2-1}(\kappa)}{B_{p/2-1}(\kappa)} - \frac{p/2 - 1}{\kappa}.$$

According to the equation below (2.6) in Baricz (2010), we have

$$\frac{B'_{p/2-1}(\kappa)}{B_{p/2-1}(\kappa)}\kappa > \kappa - 1/2,$$

for  $p \geq 4$ . Combining the above two inequalities, we have

$$\gamma_{\kappa,p} \geq 1 - \frac{1}{2\kappa} - \frac{p-2}{2\kappa} = \max\{1 - \frac{p-1}{2\kappa}, 0\}.$$

□

**Lemma C.1.** *If  $\mathbf{Z} \sim vMF_{\boldsymbol{\mu}, \kappa, p}$  and  $\kappa > 0$ , then  $E[\|\mathbf{Z} - \gamma_{\kappa,p}\boldsymbol{\mu}\|^2] = 1 - \gamma_{\kappa,p}^2$ .*

*Proof.* Let  $\mathbf{Z} = (Z_1, \dots, Z_p)^\top$  defined similarly as above. We have,

$$\begin{aligned} E[\|\mathbf{Z} - \gamma_{\kappa,p}\boldsymbol{\mu}\|^2] &= \mathbb{E}((Z_1 - \gamma_{\kappa,p})^2 + Z_2^2 + \dots + Z_p^2) = \mathbb{E}((Z_1 - \gamma_{\kappa,p})^2) + \mathbb{E}(1 - Z_1^2) \\ &= 1 - 2\gamma_{\kappa,p}\mathbb{E}(Z_1) + \gamma_{\kappa,p}^2 = 1 - \gamma_{\kappa,p}^2. \end{aligned}$$

□

**Lemma C.2.** *For a vector  $\mathbf{Z} = (Z_1, \dots, Z_p) \in \mathcal{R}^p$ , if  $\|\mathbf{Z} - \mathbb{I}_j\|_2 \leq r$  for  $0 < r < \frac{1}{2}$ , then*

$$\cos(\mathbf{Z}, \mathbb{I}_j) \geq 1 - 2r.$$

*Proof.* First, from  $\|\mathbf{Z} - \mathbb{I}_j\|_2 \leq r$ , we have  $1 - r \leq \|\mathbf{Z}\|_2 \leq 1 + r$ . Since  $\|\mathbf{Z} - \mathbb{I}_j\|_2^2 = \|\mathbf{Z}\|_2^2 + 1 - 2Z_j$ , we have

$$|Z_j - 1| = \frac{1}{2}|\|\mathbf{Z}\|_2^2 - 1 - \|\mathbf{Z} - \mathbb{I}_j\|_2^2| \leq \frac{1}{2}\{r(2+r) + r^2\} = r(1+r).$$

It follows that

$$\cos(\mathbf{Z}, \mathbb{I}_j) = \frac{Z_j}{\|\mathbf{Z}\|_2} \geq \frac{1 - r(1+r)}{1+r} = 1 - \frac{r(2+r)}{1+r} \geq 1 - 2r.$$

□

**Lemma C.3.** *For three vectors  $\mathbf{X}, \mathbf{Y}, \mathbf{Z} \in \mathcal{R}^p$ . If  $\cos(\mathbf{X}, \mathbf{Y}) \geq 1 - \alpha$  and  $\cos(\mathbf{Y}, \mathbf{Z}) \leq \beta$ , then  $\cos(\mathbf{X}, \mathbf{Z}) \leq \beta + \sqrt{2\alpha}$ .*

*Proof.* Without loss of generality, assume  $\|\mathbf{X}\|_2 = \|\mathbf{Y}\|_2 = \|\mathbf{Z}\|_2 = 1$  and  $\mathbf{Y} = (1, 0, \dots, 0)$ . Then, we know  $X_1 \geq 1 - \alpha$  and  $Z_1 \leq \beta$ . Now we consider  $\cos(\mathbf{X}, \mathbf{Z})$ . We have

$$\cos(\mathbf{X}, \mathbf{Z}) = \sum_{i=1}^p X_i Z_i \leq X_1 Z_1 + \left(\sum_{i=2}^p X_i^2\right)^{1/2} \left(\sum_{i=2}^p Z_i^2\right)^{1/2} = X_1 Z_1 + (1 - X_1^2)^{1/2} (1 - Z_1^2)^{1/2}.$$

By assumptions on  $X_1$  and  $Z_1$ , we further have

$$X_1 Z_1 + (1 - X_1^2)^{1/2} (1 - Z_1^2)^{1/2} \leq Z_1 + (1 - X_1^2)^{1/2} \leq \beta + (1 - (1 - \alpha)^2)^{1/2} \leq \beta + \sqrt{2\alpha}.$$

Combining the above two displays, we completes the proof.  $\square$

**Lemma C.4.** *To guarantee that  $\mathbf{\Pi}\mathbb{X}$  is still on the hypersphere,  $\mathbf{\Pi}$  has to satisfy the following inequality*

$$\frac{1}{\sqrt{n_k}} \leq \|\mathbf{\Pi}_{i\cdot}\|_2 \leq \frac{1}{\sigma_{n_k}(\mathbb{X}_{[G_k, :]})}, \text{ for all } i \in G_k.$$

*Proof.* The spherical requirement is  $1 = \|\mathbf{\Pi}_{i\cdot}\mathbb{X}\|_2 = \|\mathbf{\Pi}_{[i, G_k]}\mathbb{X}_{[G_k, :]}\|_2$ . On the other hand, we know

$$\|\mathbf{\Pi}_{[i, G_k]}\|_2 \sigma_{n_k}(\mathbb{X}_{[G_k, :]}) \leq \|\mathbf{\Pi}_{[i, G_k]}\mathbb{X}_{[G_k, :]}\|_2 \leq \sigma_1(\mathbb{X}_{[G_k, :]}) \|\mathbf{\Pi}_{[i, G_k]}\|_2 \leq \sqrt{n_k} \|\mathbf{\Pi}_{[i, G_k]}\|_2.$$

Thus,

$$\frac{1}{n_k} \leq \|\mathbf{\Pi}_{[i, G_k]}\|_2 \leq \frac{1}{\sigma_{n_k}(\mathbb{X}_{[G_k, :]})}$$

$\square$

## D Additional simulation results

In this section, we investigate the performance of our proposed iSphereMAP estimators in a scenario where  $p = 300$  but  $\kappa = 3000$ . This is considered as a setting with less noise in data compared to the simulation studies in Section 4 of the main manuscript.

Following Section 4, we summarize in Figure D.6 the mean squared errors (MSEs) scaled by  $p^{-1}$  of  $\widehat{\mathbb{W}}^{[1]}$  and  $\widehat{\mathbb{W}}^{[2]}$  from spherical regression and the MT method (OLS). Figure D.7 presents the performance of  $\widehat{\mathbf{\Pi}}$  estimated from our method with group information and from the MT method without group information, in terms of the match rate for one-to-one

mapping and the MSE of one-to-many mapping weight. Despite the fact that the estimators have relatively less MSE and match rate with less noise, we have the same observation as in Section 4 that the iSphereMAP procedure generally outperforms the MT method, and the refinement of  $\mathbb{W}$  reduces the MSE.

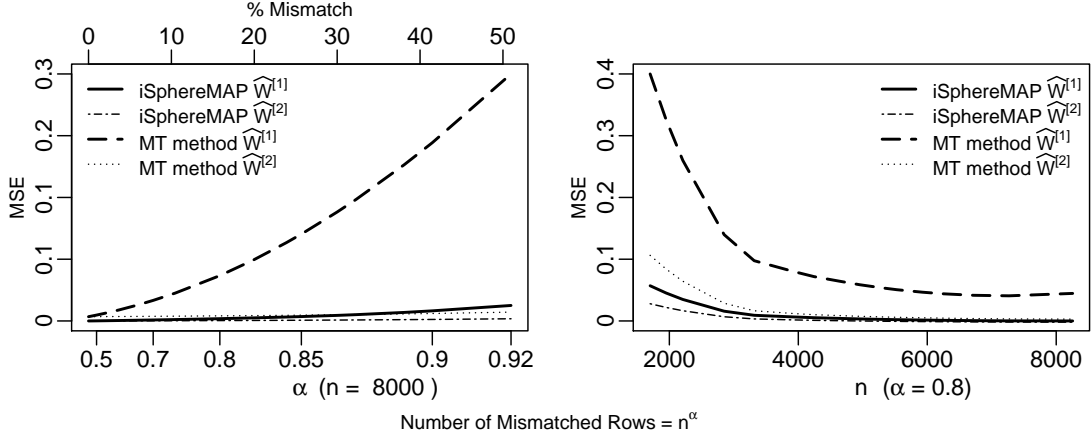


Figure D.6: Performance of  $\hat{\mathbb{W}}^{[1]}$  and  $\hat{\mathbb{W}}^{[2]}$  obtained based on the proposed spherical regression and OLS in terms of the MSE (normalized by  $p^{-1} = 1/300$ ) under ranging amount of mismatch (left panel) and sample size (right panel).

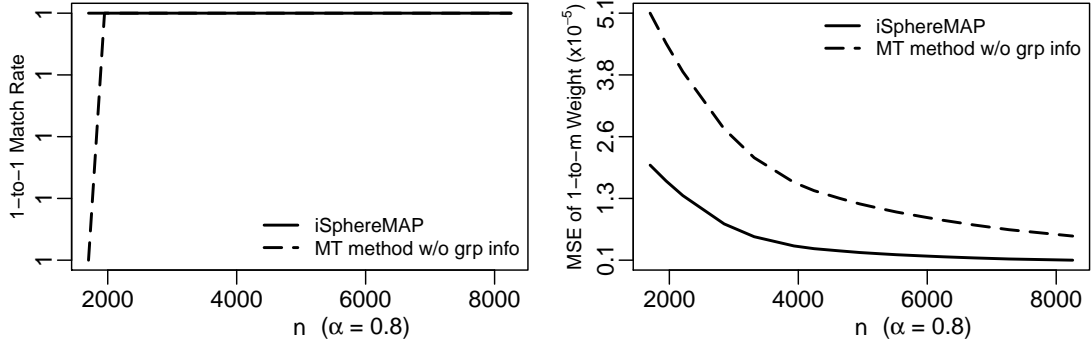


Figure D.7: Performance of  $\hat{\Pi}^{[2]}$  estimated with and without group information in terms of the one-to-one match rate (left panel) and the MSE of one-to-many weight (right panel).

## References

- Abid, A., Poon, A. & Zou, J. (2017), ‘Linear regression with shuffled labels’, *arXiv preprint arXiv:1705.01342* .
- Agency for Healthcare Research and Quality (2012), ‘Clinical Classifications Software (CCS) for ICD-9-CM’, <https://www.hcup-us.ahrq.gov/toolssoftware/ccs/ccsfactsheet.jsp>. [Online; accessed 20-August-2018].
- Austin, P. C., Daly, P. A. & Tu, J. V. (2002), ‘A multicenter study of the coding accuracy of hospital discharge administrative data for patients admitted to cardiac care units in ontario’, *American Heart Journal* **144**(2), 290–296.
- Baricz, Á. (2010), ‘Bounds for modified bessel functions of the first and second kinds’, *Proceedings of the Edinburgh Mathematical Society* **53**(3), 575–599.
- Beam, A. L., Kompa, B., Fried, I., Palmer, N. P., Shi, X., Cai, T. & Kohane, I. S. (2018), ‘Clinical concept embeddings learned from massive sources of medical data’, *arXiv preprint arXiv:1804.01486* .
- Centers for Disease Control and Prevention (2015), ‘ International Classification of Diseases, Ninth Revision, Clinical Modification (ICD-9-CM)’, <http://www.cdc.gov/nchs/icd/icd9cm.htm>. [Online; accessed 20-August-2018].
- Chang, T. (1986), ‘Spherical regression’, *Annals of Statistics* **14**(3), 907–924.
- Chang, T. (1989), ‘Spherical regression with errors in variables’, *Annals of Statistics* pp. 293–306.
- Chen, Y., Carroll, R. J., Hinz, E. R. M., Shah, A., Eyler, A. E., Denny, J. C. & Xu, H. (2013), ‘Applying active learning to high-throughput phenotyping algorithms for electronic health records data’, *Journal of the American Medical Informatics Association* **20**(e2), e253–e259.
- Chernoff, H. (1952), ‘A measure of asymptotic efficiency for tests of a hypothesis based on the sum of observations’, *Annals of Mathematical Statistics* pp. 493–507.



- Cohen, T. S., Geiger, M., Köhler, J. & Welling, M. (2018), ‘Spherical CNNs’, *arXiv preprint arXiv:1801.10130* .
- Denny, J. C., Ritchie, M. D., Basford, M. A., Pulley, J. M., Bastarache, L., Brown-Gentry, K., Wang, D., Masys, D. R., Roden, D. M. & Crawford, D. C. (2010), ‘Phewas: demonstrating the feasibility of a phenome-wide scan to discover gene–disease associations’, *Bioinformatics* **26**(9), 1205–1210.
- Di Marzio, M., Panzera, A. & Taylor, C. C. (2018), ‘Nonparametric rotations for sphere–sphere regression’, *Journal of the American Statistical Association* .
- Esteves, C., Allen-Blanchette, C., Makadia, A. & Daniilidis, K. (2018), ‘Learning so(3) equivariant representations with spherical cnns’, *arXiv preprint arXiv:1711.06721* .
- Gold, S., Lu, C.-P., Rangarajan, A., Pappu, S. & Mjolsness, E. (1995), New algorithms for 2d and 3d point matching: Pose estimation and correspondence, *in* ‘Advances in Neural Information Processing Systems’, pp. 957–964.
- Goodall, C. (1991), ‘Procrustes methods in the statistical analysis of shape’, *Journal of the Royal Statistical Society. Series B (Methodological)* pp. 285–339.
- Gotsman, C., Gu, X. & Sheffer, A. (2003), ‘Fundamentals of spherical parameterization for 3d meshes’, *ACM Transactions on Graphics (TOG)* **22**(3), 358–363.
- Gower, J. C., Gower, J. C., Dijksterhuis, G. B. et al. (2004), *Procrustes problems*, Vol. 30, Oxford University Press on Demand.
- Higham, N. J. (1986), ‘Computing the polar decomposition—with applications’, *SIAM Journal on Scientific and Statistical Computing* **7**(4), 1160–1174.
- Hsu, D. J., Shi, K. & Sun, X. (2017), Linear regression without correspondence, *in* ‘Advances in Neural Information Processing Systems’, pp. 1531–1540.
- Kaess, M. (2015), Simultaneous localization and mapping with infinite planes, *in* ‘Robotics and Automation (ICRA), 2015 IEEE International Conference’, IEEE, pp. 4605–4611.

- Kazhdan, M., Funkhouser, T. & Rusinkiewicz, S. (2003), Rotation invariant spherical harmonic representation of 3 d shape descriptors, *in* ‘Symposium on geometry processing’, Vol. 6, pp. 156–164.
- Kim, P. T. et al. (1998), ‘Deconvolution density estimation on  $so(n)$ ’, *Annals of Statistics* **26**(3), 1083–1102.
- Krive, J., Patel, M., Gehm, L., Mackey, M., Kulstad, E. et al. (2015), ‘The complexity and challenges of the ICD-9-CM to ICD-10-CM transition in emergency departments’, *The American Journal of Emergency Medicine* **33**(5), 713.
- Marques, M., Stošić, M. & Costeira, J. (2009), Subspace matching: Unique solution to point matching with geometric constraints, *in* ‘Computer Vision, 2009 IEEE 12th International Conference’, IEEE, pp. 1288–1294.
- Mathias, R. (1993), ‘Perturbation bounds for the polar decomposition’, *SIAM Journal on Matrix Analysis and Applications* **14**(2), 588–597.
- McNamee, P., Mayfield, J., Lawrie, D., Oard, D. & Doermann, D. (2011), Cross-language entity linking, *in* ‘Proceedings of 5th International Joint Conference on Natural Language Processing’, pp. 255–263.
- Mikolov et al. (2013), Distributed representations of words and phrases and their compositionality, *in* ‘Advances in neural information processing systems’, pp. 3111–3119.
- Mikolov, T., Le, Q. V. & Sutskever, I. (2013), ‘Exploiting similarities among languages for machine translation’, *arXiv preprint arXiv:1309.4168*.
- Mozer, R., Miratrix, L., Kaufman, A. R. & Anastasopoulos, L. J. (2018), ‘Matching with text data: An experimental evaluation of methods for matching documents and of measuring match quality’, *arXiv preprint arXiv:1801.00644*.
- O’malley, K. J., Cook, K. F., Price, M. D., Wildes, K. R., Hurdle, J. F. & Ashton, C. M. (2005), ‘Measuring diagnoses: ICD code accuracy’, *Health Services Research* **40**(5p2), 1620–1639.

- Paindaveine, D. & Verdebout, T. (2017), ‘Detecting the direction of a signal on high-dimensional spheres: Non-null and Le Cam optimality results’, *arXiv preprint arXiv:1711.02504* .
- Pananjady, A., Wainwright, M. J. & Courtade, T. A. (2016), Linear regression with an unknown permutation: Statistical and computational limits, *in* ‘Communication, Control, and Computing (Allerton), 2016 54th Annual Allerton Conference’, IEEE, pp. 417–424.
- Pananjady, A., Wainwright, M. J. & Courtade, T. A. (2017*a*), Denoising linear models with permuted data, *in* ‘Information Theory (ISIT), 2017 IEEE International Symposium on’, IEEE, pp. 446–450.
- Pananjady, A., Wainwright, M. J. & Courtade, T. A. (2017*b*), ‘Linear regression with shuffled data: Statistical and computational limits of permutation recovery’, *IEEE Transactions on Information Theory* .
- Papadakis, P., Pratikakis, I., Perantonis, S. & Theoharis, T. (2007), ‘Efficient 3d shape matching and retrieval using a concrete radialized spherical projection representation’, *Pattern Recognition* **40**(9), 2437–2452.
- Parle, J. V., Maisonneuve, P., Sheppard, M. C., Boyle, P. & Franklyn, J. A. (2001), ‘Prediction of all-cause and cardiovascular mortality in elderly people from one low serum thyrotropin result: a 10-year cohort study’, *The Lancet* **358**(9285), 861–865.
- Roberts, M. E., Stewart, B. M. & Nielsen, R. A. (2018), ‘Adjusting for confounding with text matching’, <https://scholar.princeton.edu/sites/default/files/bstewart/files/textmatchingfeb2018.pdf>. [Online; accessed 20-August-2018].
- Rosenthal, M., Wu, W., Klassen, E. & Srivastava, A. (2014), ‘Spherical regression models using projective linear transformations’, *Journal of the American Statistical Association* **109**(508), 1615–1624.
- Roth, J. (2016), ‘CMS’ ICD-9-CM to and from ICD-10-CM and ICD-10-PCS Crosswalk or General Equivalence Mappings’, <http://www.nber.org/data/icd9-icd-10-cm-and-pcs-crosswalk-general-equivalence-mapping.html>. [Online; accessed 20-August-2018].

- Sael, L. & Kihara, D. (2010), ‘Binding ligand prediction for proteins using partial matching of local surface patches’, *International Journal of Molecular Sciences* **11**(12), 5009–5026.
- Samarov, D., Marron, J., Liu, Y., Grulke, C. & Tropsha, A. (2011), ‘Local kernel canonical correlation analysis with application to virtual drug screening’, *Annals of Applied Statistics* **5**(3), 2169.
- Schönemann, P. H. (1966), ‘A generalized solution of the orthogonal procrustes problem’, *Psychometrika* **31**(1), 1–10.
- Slawski, M. & Ben-David, E. (2017), ‘Linear regression with sparsely permuted data’, *arXiv preprint arXiv:1710.06030*.
- Song, Y., Kimura, T., Batjargal, B. & Maeda, A. (2016), Cross-language record linkage using word embedding driven metadata similarity measurement., *in* ‘International Semantic Web Conference (Posters & Demos)’.
- Stewart, G. & Sun, J. (1990), *Computer Science and Scientific Computing. Matrix Perturbation Theory*, Academic press New York.
- Unnikrishnan, J., Haghighatshoar, S. & Vetterli, M. (2018), ‘Unlabeled sensing with random linear measurements’, *IEEE Transactions on Information Theory* **64**(5), 3237–3253.
- Wilson, B. J. & Schakel, A. M. (2015), ‘Controlled experiments for word embeddings’, *arXiv preprint arXiv:1510.02675*.
- World Health Organization (1977), *Manual of the International Statistical Classification of Diseases, Injuries, and Causes of Death. Vol. 1.*, Geneva, Switzerland.
- World Health Organization (2018), ‘ICD-11 Timeline’, <http://www.who.int/classifications/icd/revision/timeline/en/>. [Online; accessed 20-August-2018].
- Xing, C., Wang, D., Liu, C. & Lin, Y. (2015), Normalized word embedding and orthogonal transform for bilingual word translation, *in* ‘Proceedings of the 2015 Conference of the North American Chapter of the Association for Computational Linguistics: Human Language Technologies’, pp. 1006–1011.

- Yu, S., Liao, K. P., Shaw, S. Y., Gainer, V. S., Churchill, S. E., Szolovits, P., Murphy, S. N., Kohane, I. S. & Cai, T. (2015), ‘Toward high-throughput phenotyping: unbiased automated feature extraction and selection from knowledge sources’, *Journal of the American Medical Informatics Association* **22**(5), 993–1000.
- Zhou, H., Zhang, T. & Lu, W. (2014), ‘Vision-based pose estimation from points with unknown correspondences’, *IEEE Transactions on Image Processing* **23**(8), 3468–3477.